Elsevier Editorial System(tm) for Journal of Wind Engineering & Industrial Aerodynamics
Manuscript Draft

Manuscript Number:

Title: Assessing the uncertainties of using land-based wind observations for determining extreme open-water winds

Article Type: Full Length Article

Keywords: Potential wind speed; surface roughness; thermal stability;
two-layer model.

Corresponding Author: Dr. Sofia Caires,

Corresponding Author's Institution: Deltares

First Author: Sofia Caires

Order of Authors: Sofia Caires; Hans de Waal; Jacco Groeneweg; Geert Groen; Nander Wever; Chris Geerse; Marcel Bottema

Highlights

- Spatial ratios of extreme 10 meter wind speeds depend on the thermal stability
- Decreasing trends in extreme wind speed over land are due to changes in surface roughness
- Translating wind velocities to open-water requires stability and wind speed dependent roughness data
- The 10 minutes standard deviation is a better proxy from roughness than the 1 hour gust

Assessing the uncertainties of using land-based wind observations for determining extreme open-water winds

S. Caires[1], H. de Waal[1], J. Groeneweg[1], G. Groen[2], N. Wever[2] C. Geerse[3] and M. Bottema[4]

[1] Hydraulic Engineering, Deltares
[2] Royal Netherlands Meteorological Institute (KNMI)
[3] HKV Consultants
[4] Rijkswaterstaat Centre for Water Management

Abstract
For the assessment of the safety of the Dutch flood defences extreme open-water winds need to be computed. There are, however, no sufficiently long and reliable in-situ data available. On the other hand, there is a rich dataset of decades of measurements at certain coastal and relatively close by inland stations. A commonly used two-layer model for neutral atmospheres was thought to provide reasonably accurate open-water winds from the available data, given that the model assumptions seemed plausible for the extreme winds of interest. However, the model results were deemed inaccurate and not usable. Given that this was unexpected, many of the model assumptions were analysed and, with the gained further insight, their validity and contribution to the invalidity of the deemed simple model approach assessed. Our conclusion is that the quality of the model results is significantly affected by at least two aspects: the assumption of neutral stability in the model, and -equally important- the assumption of independence between the surface roughness and the wind speed.

1. Introduction

In compliance with the Dutch Water Act ('Waterwet, 2009'), the safety of the Dutch primary sea and flood defences must be assessed periodically for the required level of protection. These are typically such that flood defences will have to withstand extreme events with return periods of up to 250-10,000 years. This assessment is based on so-called Hydraulic (wave and water level) Boundary Conditions (HBC). An important component in the determination of the HBC for the water defences are the statistics of the natural variables that, directly or indirectly, may cause the water defences to fail. One of such natural variables is the surface wind speed. More specifically, in order to force the wave and flow models used for the determination of the HBC, information is required on wind conditions over open-water areas, pertaining to return periods of up to thousands of years. This information needs to be derived from several sources.

Currently, the main source of reliable and validated information is wind data measured at the wind stations of the Royal Netherlands Meteorological Institute (KNMI). However, these data cover at most 50 years, which means that statistical extrapolation is required. Moreover, most measurement stations, and especially those for which decades of data are available, are located at land, typically several tens of kilometres away from the centre of the considered open-water areas, like the North Sea, the Lake IJssel and the Wadden Sea, see Figure 1. This means that spatial interpolation and extrapolation of wind information is required, taking account of transitions from land to water and vice versa.

In earlier assessments of the HBC, the wind modelling concept developed by Wieringa and Rijkoort, referred to as the *Wieringa-Rijkoort two-layer model (*WRTL model), was used to provide the required spatial information (Wieringa and Rijkoort, 1983; see also Wieringa, 1986). Wieringa (1986) defines two layers for his WRTL model: a surface-layer up to 60 m height in which a local roughness is valid, and an upper (or Ekman) layer stretching to the top of the boundary layer, in which an average meso roughness for a 5x5 km surface patch is valid. If the local and meso roughness are equal (i.e. for sufficiently homogeneous terrain), the WRTL model reduces to the well-known theoretical concept of logarithmic surface-layer profile plus resistance law. The main assumptions of the WRTL model are neutral stability when minimal average wind speed over land is at least 6 m/s and independence between the surface roughness and the wind speed. Using these assumptions and including

characteristics of the measuring chain, the directional dependent upstream local surface roughness is calculated for translation of measured wind to so-called potential wind.

Wieringa (1986, 1996) defines the *potential wind speed* is a standardised speed corrected for local roughness effects, representing the 1 hour averaged wind speed at 10 metres height at a location with a local roughness of 3 cm, corresponding to short grass. From these series of potential wind, extreme value statistics are applied on independent peak-over-threshold values. One of the implications of the model assumptions is that if at some value of the return period T, the wind speed return value at location A is larger than at location B, then the wind speed return value at location A is larger than at location B *for all values of T.*

However, as illustrated in Figure 2, when comparing omni-directional extreme potential wind velocities from coastal and inland stations, the higher potential wind velocities for the inland stations exceed those for the coastal stations. When fitting through the data, the return value lines cross each other and for longer return periods the estimates for inland stations are higher than for the coastal stations, which cannot be explained by the WRTL model. The stations used here to illustrate the problem were the coastal station Hoek van Holland and the inland station Soesterberg, but such discrepancies are also found when analysing other station combinations. Further (often similar) indications of discrepancies between data and the WRTL model can be found in the storm wind speed measurements analysed by Taminiau (2004), Bottema (2007, p. 184), Tieleman (2008) and Bottema and Van Vledder (2009). Note that these discrepancies also occur for cases with (nearly) equal local and meso roughness lengths at a given location.

This discrepancy between the data and the modelling concept, the WRTL model, has been named the “curvature problem” (alluding to the difference in curvature, shape, between the return value lines of data from inland and coastal stations). The aim of the present study is to identify and analyse potential causes for the curvature problem. We focus on identifying what is the effect of some assumptions made in the standardization of the measured wind speeds into potential wind speed and in the translation of these to 10 m wind speeds to other, preferably open-water, locations.

The context and implications of the curvature problem are described in detail in the next section. In Section 3 we report on our investigations on the possible causes of the curvature problem. This article ends in Section 4 with conclusions and recommendations.

The main data used in this study are the time series of the wind velocity measurements (De Haij, 2009) and the respective time series of potential wind speed at the KNMI wind stations, see Figure 1 and Table 1.

Note that another possible source of information for deriving extreme wind conditions over open-water areas is data from meteorological models on a high temporal and spatial resolution. The validation and usage of such data are foreseen in the next safety assessment (probably in 2017) of the Dutch primary sea and flood defences.

2. Basic concepts and the curvature problem

2.1 Introduction

In this section the context and implications of the curvature problem are described. We start in Section 2.2 by describing the general two-layer model concept. In Section 2.3 we describe the application of this concept in the WRTL model, the potential wind concept, the estimation of the roughness lengths and how the WRTL model is used to compute wind characteristics at locations other than the locations of the wind stations. The roughness lengths are needed for the determination of the potential wind and application of the WRTL model. Having described all the background of wind modelling, Section 2.4 provides a more concrete description of the curvature problem.

2.2 The basic two-layer model concept

The planetary boundary layer is often divided in *two-layers*: the surface layer, which occupies the lowest 10% going from the surface up to about 10-100 m, and the Ekman layer, whose

lower limit oscillates below approximately 100 m height and the upper limit oscillates between about 100 m–2 km.

In the surface layer, under conditions of horizontal homogeneity and stationarity, the Monin-Obukhov theory (Foken, 2006) can be applied. In this layer it is assumed that the wind does not change direction and a non-adiabatic process is verified. On such conditions the flow in the surface layer is defined by non-adiabatic wind and temperature profiles (Businger et al., 1971). The surface layer profile expressions can be greatly simplified by a null vertical potential temperature gradient: a neutral atmosphere. In such situation the wind velocity *U* (m/s) at a height *z* (m) in the surface layer is given by (Tennekes, 1973)

$$U_z = \frac{1}{\kappa} u_* \ln\left(\frac{z}{z_0}\right), \quad (1)$$

where u_* (m/s) is the friction velocity, $\kappa \sim 0.4$ the von Kármán constant (Frenzen and Vogel, 1995), and z_0 (m) is the surface roughness. Here $\ln$ denotes the natural logarithm. Above land the surface roughness can be estimated by visual inspection, or using land-use maps, or using turbulence proxies such as the wind velocity maxima (the gust) or, when available, directly the standard deviation of the wind velocity or from the vertical wind speed profile. Above water the surface roughness is often assumed to be given by

$$z_0 = \alpha \frac{u_*^2}{g}, \quad (2)$$

where $g = 9.81\, m/s^2$ is the acceleration due to gravity and α is the Charnock 'constant'. Different estimates for α exist, varying from 0.004 to 0.032 (see e.g. Komen et al., 1994).

Since the development of two-layer models weather predictions models have been developed which include many of the relevant processes explicitly.

2.3 The Wieringa-Rijkoort two-layer model

The concept of a two-layer model is since the work of Wieringa and Rijkoort (1983) and Wieringa (1986) used in the analysis of Dutch surface wind measurements. This two-layer model is used for the definition of the potential wind and in the horizontal (spatial) transformation of wind characteristics. The main model characteristics are schematized in Figure 3. The term macro wind used for the wind velocity in the free atmosphere (cf. Figure 3) was introduced in this context to acknowledge the fact that it may differ from the geostrophic wind. In an ideal situation the wind transformed in the two-layer model to the top of the Ekman layer (the macro wind) will be close to the geostrophic wind in the lowest layer of the free atmosphere, but will in fact be influenced by other effects than only the pressure gradient and the Coriolis force.

The specifics of the model are as follows:

1. Neutral stability is assumed. According to Wieringa and Rijkoort (1983, p. 51) in the surface layer stability effects are only relevant for wind speeds below 6 m/s. Such low wind speeds are not relevant for extremes and therefore not accounted for in the model.
2. The blending height, the height of the top of the surface layer, is fixed at a value of 60 m (see Wieringa and Rijkoort, 1983 and Verkaik, 2000).
3. A schematized relation between the (upwind) surface roughness and the wind in the two layers is applied, see right panel of Figure 3. The upwind surface roughness is schematized by two single roughness parameters, each governing the wind properties in one of the two layers in the model:
    - The meso-scale roughness is a representative value for a relatively large upwind area (5x5 km, Wieringa, 1986) and governs the wind properties in the Ekman (= upper) layer.
    - The local roughness is a representative value for a relatively small upwind area (100-500 m) and governs the wind properties in the surface (= lower) layer.
4. The meso wind is assumed not to depend on the local roughness. I.e., the effects of all surface inhomogeneities have blended into the mean flow.

5. In the Ekman layer the Ekman spiral formulae are not used, but geostrophic drag relationships (cf. Garrat, 1992, Section 3.2.3 and Wieringa, 1986). Accordingly, the wind speed in the free atmosphere, the *macro wind speed*, S_h, can be obtained from

$$S_h = \sqrt{U_h^2 + V_h^2}\ , \qquad (3)$$

where $U_h = \frac{u_{*m}}{\kappa}\ln\left(\frac{h}{z_{0m}}\right) = \frac{u_{*m}}{\kappa}\ln\left(\frac{u_{*m}}{fz_{0m}} - A\right)$, $V_h = B\frac{u_{*m}}{\kappa}$,

z_{0m} (m) is the meso-scale roughness length, $h = u_{*m}/\left(f \cdot \exp(A)\right)$ (m) the height of the upper boundary of the Ekman layer (the height of the planetary boundary layer), *f* is the Coriolis parameter ($1.14*10^{-4}$ s^{-1}, for the Netherlands), A=1.9 and B=4.5 are empirical constants (Wieringa, 1986, p. 876) and u_{*m} (m/s) is the meso-scale friction velocity.

The potential wind speed, a fictitious local wind speed at 10 m height, is used in this model to describe the surface wind speed. It is the local wind speed which would have occurred at a specified location if the local (not necessarily the meso) roughness length would have been 0.03 m. It can be computed from a wind measurement in the surface layer, on the basis of the WRTL model described above, once the local roughness is known, see Wieringa (1996, Figure 1). The ratio between the potential wind speed and the measured wind speed at a height *z*, the so-called exposure correction factor, *ECF*, is, according to assumptions 1., 2. and 4. above, given by:

$$ECF = \frac{U_p}{U_z} = \frac{\ln(10/0.03)}{\ln(60/0.03)}\frac{\ln(60/z_0)}{\ln(z/z_0)}\ . \qquad (4)$$

There are a number of reasons why it is useful to convert measured wind into potential wind (cf. Wieringa, 1996). First, it is the wind that would be measured by ideal stations according to the World Meteorological Organization (WMO) specifications. An ideal station is located in an unobstructed area, which can be interpreted as having a local roughness of 3 cm (the roughness length of an open grass area), and at a measurement height of 10 m (in accordance with WMO-requirements). Second, inhomogeneities in the data due to changes in the measurement surroundings and in anemometer height can be removed. For climatological studies it is important that the data time series are not affected by changes in local roughness, since they may be wrongly interpreted as climatic trends and\or variations.

Given that measured wind speeds need to be converted into potential wind speeds, an important parameter in the application of the WRTL model is the local surface roughness. As mentioned before, given the present single height-level measurements, it can be estimated either from the turbulence in the measurements or from land-use maps (cf. Verkaik, 2001, 2006).

For the locations where measurements are available, the KNMI wind stations, the local roughness is estimated from the turbulence assuming again neutral stability for average hourly wind speeds over land of at least 6 m/s. In the neutral limit $\sigma_u/u_* = c \approx 2.2$ (Verkaik, 2000). This assumption in combination with Eq. (1) yield the roughness length. However, since records before 1995 of wind speed for the Netherlands did not include the standard deviation, the potential wind speed time series considered by Wieringa and Rijkoort (1983) were computed using the median of the maximum gust over one hour from series of about three years to estimate the surface roughness, see Verkaik (2000). This is done per 20 degree wind direction sector for all stations without major terrain of site changes.

Note that in the turbulence analysis the surface roughness is assumed to be independent of the wind speed (even for stations above water) and, if the station is not moved, the estimated roughness lengths and associated ECFs are determined over a period of three consecutive half-year winters or half-year summers based on the mean values for those periods (see Wever and Groen, 2009). This three year period is chosen such that there is for practically every station and every wind direction sector enough data to reliably estimate the gustiness.

For locations where no surface wind speed measurements are available, roughness lengths are computed from land-use and orography maps by modelling the drag coefficients at the blending height. Land-use maps are raster files with a given resolution and to each pixel a land-use class is assigned. Classifications such as the Davenport terrain roughness classification (Wieringa, 1993) can be used to assign a roughness length to each land-use class. Local and meso-scale roughness lengths have been computed covering the whole of the Netherlands by Verkaik (2001). Note that for locations where surface wind speed measurements are available, only local roughness is calculated from turbulence, meso-scale roughnesses cannot be obtained from turbulence analysis and its estimation requires information from land-use maps.

As mentioned before, the locations of interest for the present case (for HBC-evaluation) do not generally coincide with those where KNMI wind climatologies have been measures. Worse still, most locations of interest are over open-water, while most KNMI-locations are land-based. The WRTL model can in principle be used to derive the (unknown) wind speed at a certain location from the wind at a nearby location where the wind speed is known. For both locations the roughness values must be known. For short distances (up to some kilometres, Wieringa and Rijkoort, 1983, p. 79 and Wieringa, 1986, p. 875) the meso wind speed was assumed equal for both locations. For longer distances (up to some tens of kilometres) the macro wind was assumed equal for both locations.

2.4 The curvature problem

The Wieringa and Rijkoort two-layer model assumptions have the following implications:

> Consider the wind speed return levels at two locations, A and B, in the Netherlands.
>
> If at some value of the return period T, the wind speed return level at location A is larger than at location B, then the wind speed return level at location A is larger than at location B for all values of T. In other words: the lines of the wind speed probability of exceedence at A and B should not cross.
>
> More precisely:
>
> Not only should the wind speed return levels at location A always be higher than those at location B, also the ratio of the wind speed return level at location A and B should (approximately) be constant for all values of T. In other words: the lines of the wind speed probability of exceedence at A and B differ only by (about) a constant factor on the wind speed levels; the lines have (approximately) the same shape (curvature).

This is, however, not confirmed by the data shown in Figure 2. In fact, the figure shows that under moderate conditions the wind speeds at Soesterberg are considerably (~20%) lower than the wind speeds at Hoek van Holland and that under extreme conditions the wind speeds at the inland station Soesterberg exceed those at the coastal station Hoek van Holland.

3. Investigation of possible causes for the curvature problem

3.1 Introduction

In this section we investigate possible causes for the curvature problem, looking into the processing of the data and the validity of the WRTL model assumptions.

We focus on identifying what is the effect of the assumptions made in a) the standardization of the measured wind speeds into potential wind speeds and in b) the translation of these to 10 m wind speeds at other locations. We investigate:

1. To what extent the curvature problem is potentially due to the exposure correction factors (ECFs) used in the conversions from raw to potential winds (Section 3.2).

2. Whether the applied ECFs have indeed produced homogeneous (free of local roughness effects) potential wind speed time series, by checking whether jumps and/or trends can be identified in the time series (Section 3.3);
3. Inaccuracies in the ECF estimates due to uncertainties in the anemometer height (Section 3.4);
4. To what extent ignoring the variation of the sea roughness variation with wind speed when computing the ECF and translating data from one inland location to an open-water location may reproduce curvature differences (Section 3.5).
5. The role of storm dynamics: although the curvature problem pertains to wind statistics, it may be worthwhile analyzing some physical spatial details of observed extreme storm events, since data from these extreme events will have a large impact on the statistics (Section 3.6).
6. Whether spatial gradients in the wind speed show any preference for the time of the day, using time of the day as a proxy for stability and look at additional indications of non-neutral stability in the data, in order to identifying to what extent the curvature problem results from the neutral stability assumption made when transforming the data from one location to another (Section 3.7).

Note that in 1. to 3. we concentrate on the effects due to the standardization of the measured wind speeds into potential wind speeds and in 5. and 6. due to the translation of these to 10 m wind speeds at other locations, in 4. we consider both.

3.2 Analysis of the ECF

As a first step, it was investigated to which extent the curvature problem is potentially due to the ECFs used in the conversions from raw to potential winds. As mentioned before, the ECFs were evaluated from the gustiness of the wind. It was found that the wind gustiness and especially the maximum wind gust of 1 hour samples are not solely due to the surface roughness, but also due to thermal effects, especially in northwesterly flow in the winter (Wever and Groen, 2009). This effect introduces wind direction-dependent errors in the calculation of the ECFs. In Wever and Groen (2009), a method was developed to calculate the ECFs by making use of measurements of the 10-minute wind standard deviation to relate ECFs based on 1 hour gustiness analysis to ECFs based on 10 minute wind standard deviation. The correction of the ECF has lead to a reduction of typically 1-5% downward revision of exposure corrected winds over land, with a maximum of 15-20% on individual measurements with large upstream roughness (cf. Wever and Groen, 2009, Figure 4.5.1). The latter locations are generally not used as HBC-related reference locations for wind. As a result, when recreating Figure 2 using the new potential wind speed data, as shown in Figure 4, yields only a small reduction of the curvature problem. The main conclusion from this analysis is that the above-described errors in former ECF estimates (by now they are corrected following Wever and Groen, 2009) contribute only marginally to the curvature problem.

3.3 Inhomogeneities and trends

In order to check the stationarity of the data, linear fits were performed to the annual mean time series of wind speeds above 5 m/s. The standard Mann-Kendall non-parametric test was used to identify the significant results -namely the existence of trends- at a 5% level. The results are shown in Table 1. For some of the stations considered in Table 1, trends in the annual maxima of potential wind were also computed (not shown), these are generally negative and with a higher (absolute) magnitude than the corresponding trends in the annual means. Furthermore, in the time series of the measured and potential wind speeds (not shown) it can be seen that in some cases jumps in the measurements are also to be found in the potential wind data. These trends and jumps indicate that the data are not fully homogeneous (see also Verkaik et al., 2003a, Section 2.5) and/or that significant changes in meso-scale roughness have occurred (Wever, in preparation). Nevertheless, from the analysis of the data it can be concluded that for many stations the potential wind time series are more homogeneous (less prominent trends and jumps) than the measurement time series (cf. Table 1).

Wever (in preparation) shows that the trends in surface wind speeds are mainly caused by an increase in surface roughness (see also Vautard et al., 2010) and that the increase in local

surface roughness is likely to be accompanied by an increase in meso-scale roughness as well. Wever (in preparation) results extend the work by Smits et al. (2005), where trends in peak wind speeds were found that could not be supported by changes in geostrophic wind, calculated from pressure measurements (using stations De Bilt, De Kooy and Eelde) or reanalysis data.

Here, the analysis of Smits et al. (2005) is repeated using the corrected (Wever and Groen, 2009) potential wind time series for the extended period 1962-2008. Our results closely resemble those of Smits et al. (2005) in terms of spatial pattern, the trends differ as a consequence of different periods, methods and/or data being used. Figure 5 compares the trends in moderate wind events (occurring on average 10x per year) identified here and by Smits et al. (2005).

As in Wever (in preparation), we correlated the trends in peak potential wind speeds with trends in the exposure correction factors per station. The trend in the exposure correction factors is determined by averaging the directional trends, using the relative frequency of events from a specific wind direction as weights. Figure 6 shows the trend in wind events (% per decade) versus the trend in exposure correction factors (% per decade), for the earlier classified weak (occurring on average 30x per year), moderate and strong (occurring on average 2x per year) wind events, respectively. These figures suggest that trends in peak wind speeds can also be explained by trends in surface roughness.

3.4 Non-stationary anemometer height

The estimates of the ECF and associated potential wind speeds may be affected by inaccuracies in the data processing due to uncertainties in the anemometer height. The measurements above water and at some of the coastal stations will in some situations be affected by variations of the still water level (SWL), the combination of both the tidal and the storm effects.

For the storm surge situations, let us consider the example of the Hoek van Holland station at 15 m height, which is located at a pier, almost 100 m from the mainland. The pier is in a region where storm surges can be quite high. For instance the 1 in 10,000 and 1 in 100 year return values of the SWL in the region are of approximately 5 m and 3 m respectively, according to Dillingh et al. (1993). Since the procedure to compute the ECF does not consider a SWL other than zero the computed ECF and potential wind speed will for extreme water levels, which generally accompany extreme sea wind speeds, be underestimated. Such inaccuracies not only affect the height correction of the wind speed, but also the roughness length estimates.

Table 2 shows for a number of wind speed measurements at the station height of 15 m the relation between the ECF assuming that the SWL is zero and for the case of a SWL of 3 and 5 m. The roughness lengths have for this example been estimated using eqs. (1) and (2). Two values were considered for the Charnock constant: 0.018 and 0.032. The underestimation is slightly higher when considering the higher Charnock constant value. The underestimation when converting a wind speed measurements of 20 m/s to potential wind speed is about 2.5% and 5% when the SWL is 3 and 5 m, respectively. When considering a SWL of 1 m (not shown) the underestimation is approximately 0.8 %.

When considering the tidal influence only, the wind at low tide is overestimated, and the wind at high tide is underestimated. The difference between high and low tide at key locations along the Dutch coast varies between 1.4 and 3.8 m (Dillingh et al., 1993, Fig. 2.1). Given these tidal ranges, it can be concluded that the influence of the tide on the potential wind speed varies between ±1%.
Note that in the estimates presented stability effects are not accounted for, even though they may be non-negligible in practice (for especially stable atmospheres), see Verkaik (2000, Fig. 12).

3.5 Effect of wind speed dependent surface roughness of water

3.5.1 Introduction

One of the basic assumptions within the current application of the two-layer model is that the values for the local and the meso-scale roughness length are fully determined by the (upwind) surface roughness characteristics and *do not depend on the wind speed*. For locations nearby large water areas, this assumption is actually invalid: it is rather well known that the surface roughness of a water area varies with wind speed.

In this section, we assess to what extent the curvature problem may be attributed to the wind speed dependency of the water roughness (see also Verkaik et al, 2003a, Section 8.5.1). The approach is described in Section 3.5.2. Section 3.5.3 presents the computational results and discusses its implications.

3.5.2 Approach

As part of the general approach, the statistics of potential wind are considered to be fully determined by the macro wind statistics and the roughness characteristics (i.e. the local and meso-scale roughness). In addition, the macro wind statistics are supposed to vary little and smoothly over the Netherlands. As part of the simplified approach in the current section, the macro wind speed return levels at Soesterberg and Hoek van Holland are assumed to be equal.

With this assumption, we can assess the effect of the difference in roughness characteristics on the statistics of the potential wind. In order to analyse this effect, we study the relationship between couples of wind speed values at several recurrence intervals. The relationship between the potential wind speed return levels at Soesterberg and Hoek van Holland is derived from the data and fits as presented in Figure 2, leading to Table 3 and Figure 7.

Note that Figure 7 includes two vertical axes, having different colours: the black lines in the figure (both solid and dashed) are related to the left y-axis (which is black too), whereas the red lines in the figure (both solid and dashed) are related to the right y-axis (which is red too). In this figure, the *curvature difference* as shown in Figure 2 may be recognized in two ways: a) the solid black line is not a straight line through 0 and b) the solid red line is not horizontal, in fact the slope of the red line may be regarded as a measure of difference in curvature: a steeper slope refers to a larger curvature difference. The crossing of the two lines as shown in Figure 2 may also be recognized in Figure 7 in two ways: a) the solid black line crosses the dashed black line and b) the solid red line crosses the dashed red line.

Here we assess to what extent the WRTL model may reproduce a relationship between the potential wind at two different locations as shown in Figure 7, when we apply a wind speed dependent surface roughness at one of the locations.

The basic application of the WRTL model is to assess the local wind speed at an arbitary location of interest B (typically over open-water) from the local wind speed at (an inland) location A, for known roughness conditions at both locations; see the red arrows in Figure 8. Note that the direction of the chain of arrows in Figure 8 does not refer to a physical chain of causes and effects, but just to an order of computation used here, using the formulas given in Section 2.

In the present study we consider the following academic situation. The macro wind speed at location A ($S_{h,A}$) is considered to be equal to the macro wind speed at location B ($S_{h,B}$). Any difference in wind direction due to differences in roughness between location A and B is ignored. Location A is situated on land. The roughness of surrounding area is homogeneous. The local roughness length $z_{0,A}$ and the meso-scale roughness length $z_{0m,A}$ are both equal to 0.2 m. Location B is surrounded by a large area of water. The local roughness length $z_{0,B}$ and the meso-scale roughness length $z_{0m,B}$ are considered to be equal. Note that the WRTL model largely reduces to the basic theoretical framework of logarithmic wind profile and resistance law as long as local and meso roughnesses do not differ from each other.

Furthermore, we shall consider two situations at the open-water location (location B). First, a wind speed independent roughness, with a roughness length of 2 mm. Second, a wind speed dependent roughness according to Eq. (2) with a Charnock constant α equal to 0.032.

As presented in Figure 8, a potential wind may be computed following two different approaches, which are identified as: 'potential wind based on meso wind (U_p)' (turquoise arrows in Figure 8) and a 'potential wind based on local wind (U_{pc})' (green arrows in Figure 8). In this second approach, the potential wind, $U_{pc,}$ is derived from the local wind speed using the (local) ECF, which does not depend on the wind speed (see third paragraph from the end of Section 2.3). When a wind speed dependent roughness is applied for computing U_p at location B (in the above mentioned second situation), U_p differs from U_{pc}.

A representative value for the ECF is required in order to derive the potential wind from the local wind, which is here assumed to be at 10 m. For location A, a representative value for the exposure correction factor follows from Eq. (4):

$$ECF_A = \frac{U_{p,A}}{U_{10,A}} = \frac{\ln\left(10/z_{0,ref}\right)}{\ln\left(60/z_{0,ref}\right)} \cdot \frac{\ln\left(60/z_{0,A}\right)}{\ln\left(10/z_{0,A}\right)} = \frac{\ln(10/0.03)}{\ln(60/0.03)} \cdot \frac{\ln(60/0.2)}{\ln(10/0.2)} = 1.11 \,. \tag{5}$$

For location B, the representative value for the ECF depends on the considered situation. In the first situation (i.e. wind speed independent roughness) the value follows from:

$$ECF_B = \frac{U_{p,B}}{U_{10,B}} = \frac{\ln\left(10/z_{0,ref}\right)}{\ln\left(60/z_{0,ref}\right)} \cdot \frac{\ln\left(60/z_{0,B}\right)}{\ln\left(10/z_{0,B}\right)} = \frac{\ln(10/0.03)}{\ln(60/0.03)} \cdot \frac{\ln(60/0.002)}{\ln(10/0.002)} = 0.93 \tag{6}$$

In the second situation (i.e. wind speed dependent roughness) however, the ratio of potential wind and local wind is not constant: the ratio depends on the local roughness, which in its turn depends on the local wind speed. In other words: whereas the real water roughness depends on the wind speed, its effect is corrected for by a constant (i.e. wind speed independent) ECF. In this study, a representative value for the ECF is based on the average value for local wind speeds ranging from 5 to 12 m/s:

$$U_{10,B,i=1..8} = [5,6,7,8,9,10,11,12] \tag{7}$$

$$ECF_B = \frac{1}{8}\sum_{i=1}^{8} \frac{U_{p,B}\left(U_{10,B,i}\right)}{U_{10,B,i}} = 0.90 \tag{8}$$

The relationship between $U_{p,B}$ and $U_{10,B,i}$ follows from Eq. (2), with $\alpha = 0.032$ (Verkaik et al., 2003a).

The values for the ECF, as presented in eqs. (5) and (8), show a fairly good agreement with the results from gustiness analysis for Soesterberg and Hoek van Holland for NW wind direction (Wever and Groen, 2009, Figs 4.1.1 and 4.1.3).

3.5.3 Computational results and analysis

The results to be presented next were computed as follows. First consider a series of values for $U_{10,A}$, ranging from 1 to 40 m/s. Second, for every value of $U_{10,A}$, compute the associated values of $U_{pc,A}$ using ECF_A, compute $U_{10,B}$ following the red arrows in Figure 8, and compute $U_{pc,B}$, using the computed $U_{10,B}$ (from $U_{10,A}$) and ECF_B. Third, analyse the following relationships (both presented in a graph similar to Figure 7): $U_{10,A}$ vs. $U_{10,B}$ and $U_{pc,A}$ vs. $U_{pc,B}$.

Figure 9 shows the relationship between the *local wind* at locations A and B, according to the two-layer model using a *wind speed independent water roughness* (i.e. just following the red arrows in Figure 8 with $z_{0A}=z_{0mA}=0.2$ m and $z_{0mB}=z_{0B}=0.002$ m). The local wind at location B turns out to be much larger than at location A. The ratio of the wind speeds although slightly increases with increasing wind speed, due to the non-linearity of the two-layer model, is almost constant. The found relations are in accordance with the implications of the Wieringa and Rijkoort two-layer model assumptions described in Section 2.4.

Figure 10 shows the relationship between the *local wind* at locations A and B, according to the two-layer model using a *wind speed dependent water roughness (*i.e. just following the red arrows in Figure 8 with $z_{0A}=z_{0mA}=0.2$ m and $z_{0mB}=z_{oB}$ and being given by Eq. (2)*)*. The

local wind at location B still turns out to be much larger than at location A. But in this case the ratio of the wind speeds strongly decreases with increasing wind speed, i.e. there is a difference in curvature. These observed relationships agree with the expectations. They follow from the fact that the roughness at location B increases with increasing wind speed but remains considerably smaller than the roughness at location A (which does not depend on the wind speed).

Figure 11 shows the relationship between the *potential wind* (derived from local wind) at locations A and B, according to the two-layer model, using a *wind speed dependent water roughness* when computing $U_{10,A}$ from $U_{10,B}$, i.e. using the $U_{10,A}$ and $U_{10,B}$ presented in Figure 10 and multiplying then by ECF_A=1.11 and ECF_B=0.90, respectively, to obtain $U_{pc,A}$ and $U_{pc,B}$. In Figure 11, the difference in curvature is similar to the one in Figure 10, but the wind speed ratios are smaller than in Figure 10, bringing the relationships of Figure 11 closer to those in Figure 7. However, the curvature difference is still considerably smaller than in Figure 7.

Our results show thus that the wind speed dependency of the water roughness explains to a certain extent the curvature problem. The curvature is present when making z_{0mB} and z_{0B} to depend of the wind speed (Figure 10) and is even more accentuated when also using wind speed independent ECF (Figure 11). However, although the lines for the potential wind come remarkably close to each other, it does not reproduce crossing lines within the range of computed conditions. If we where to equal ECF_A to 1.25 (corresponding to a roughness length of 0.6 m, or equivalently ECF_B to 0.8, z_0=1e-13) the lines would in fact cross each other, but such roughness lengths are not realistic. One can, therefore, conclude that the fact that the water surface roughness is not constant, but depends on (a.o.) the wind speed, appears to provide a significant part (but certainly not all) of the explanation for the difference in curvature.

Note that the above presented study focuses on a purely academic situation consisting of two locations having a homogeneous upwind surface roughness. Taking account of the non-homogeneity of the upwind surface roughness may yield results (relationships) in which the different upwind roughness conditions of land versus water are less clearly pronounced than in the present analysis. Furthermore, a rather high value for the Charnock constant (0.032) is used. This high value yields a relatively strong increase of the drag with increasing wind speed, which may yield a relatively strong difference in curvature. In the Lake IJssel area, e.g., a Charnock constant of 0.018 was found to be most representative (Bottema, 2007). If such a lower constant would have been applied in this analysis, the resulting difference in curvature would have been less pronounced. Finally, it should be noted that the water surface roughness actually depends on the water surface characteristics; a combination of waves, varying from ripples to wind waves and swell, propagating at different speeds in (slightly) different directions. It is not clear which surface characteristics are decisive for the roughness value. In general, however, there is a rather strong relationship between the wind speed over the water and the surface characteristics. This relationship provides the opportunity to consider the wind speed over the water area as a proxy for the water surface characteristics, and to relate the surface roughness to the wind speed. Nevertheless, it should be kept in mind that the water surface characteristics do *not only* depend on the wind speed. Especially in coastal areas, where waves are affected by bottom changes and decreasing water depths, the applicability of Eq. (2) to estimate the roughness length is disputable.

At first sight it seems to be rather easy to (at least) significantly reduce or explain the curvature problem by implementing an approximating relationship between the wind speed and the water surface roughness, both in the transformation of measured wind to potential wind and in the transformation from one location to another. However, this will not be straightforward in sites near water areas, such as coastal site, in which the water roughness is only relevant for certain well defined wind directions.

3.6 Storm dynamics

In this section we look at the spatial distributions of storms. Although not showing the figure, we have investigated to which extent the features seen in Figure 4 (and equivalently in Figure 2) can be explained by storm dynamics: by restricting the empirical distributions in Figure 4 to the same time period, directional sector and storm instants. The conclusion was that the

curvature problem was always prominent in the resulting, restricted, empirical distributions. We look further at the spatial pattern of the most extreme storms available.

For the determination of the extreme (not reported here, see Caires, 2009) and mean wind climate, we have tried to find a period of at least 30 years in which data from a maximum number of stations would be available with a good coverage of the period considered. The period chosen was 1970 until 2008 (39 years) and as much as 21 stations can be considered in that period (cf. Figure 1), namely, IJmuiden, Texelhors, De Kooy, Schiphol, De Bilt, Soesterberg, Leeuwarden, Deelen, Lauwersoog, Eelde, Twenthe, Cadzand, Vlissingen, L. E. Goeree, Hoek van Holland, Zestienhoven, Gilze-Rijen, Herwijnen, Eindhoven, Volkel and Beek.

Considering these stations, the highest 20 potential wind speed storm peaks from 1970 until 2008 were selected. For each storm represented in those peaks, the stations with peaks within that storm were identified. The criteria for belonging to the same storm was that the peak values were within the same 12h interval (this was found to be no restriction, since storm peaks in the available stations generally are within periods shorter than 9 hours). The identified storms were ranked from higher to lower in terms of the maximum peak potential wind speed within the storm. A total of 107 storms were identified in terms of potential wind speed.

Figure 12 shows the spatial pattern of the top four potential wind speed storms. The numbers indicate the ratio between the peak potential wind speed at the indicated station and the maximum at other stations in that storm, but not necessarily at the same instant. The blue arrows indicate the wind direction of the peak wind speed at the considered station. The red dots mean that the considered storm was not within the top 20 peaks of the considered station.

The figure shows that the spatial gradients and directional patterns vary considerably from storm to storm. For the 1st storm Figure 12 shows that at the peak the wind directions in the coastal and northern stations are from the Northwest, whereas in the inland stations south of the IJsselmeer they are from the West. For the 4th storm Figure 12 shows that the highest peak is in the inland station Schiphol. The highest three storms are defined by the potential wind speed in Texelhors.

Analysing all identified storms (not shown) one sees that spatial coverage, pattern and gradients of the extreme storms may vary significantly. In fact, ratios of peak coastal and land potential wind speed close to one seem to systematically occur in extreme storms and are in specific situations even lower.

In conclusion we can say that extreme storm maxima can be rather localized and the stations affected by a certain storm can vary substantially from storm to storm. This indicates that spatial variations of the geostrophic wind and pressure fields changing in time (causing isallobaric winds) are not uncommon in extreme storms, and that a model assuming a smooth gradient in geostrophic wind, decreasing from the coast to inland between two stations does not properly describe such storms. I.e., we observe that storm characteristics vary over individual storms and that storms only touching one or two stations also implicate non-stationary geostrophic wind patterns and other effects. This is a complicating factor for extreme statistics. Furthermore, when data selection is applied (for example: measurement period, directional sector) there is the possibility that data sampling effects affect the results.

3.7 Thermal (stability) effects

3.7.1 Introduction

In the WRTL model neutral atmospheric stability is assumed, i.e. that in the surface layer there is no vertical potential temperature gradient and therefore a logarithmic vertical wind profile can be assumed. According to Wieringa and Rijkoort (1983, p. 51): “effects of stability on the wind profile in the lower tens of metres of the atmosphere become important only when the wind speed at 10 m height is lower than 6 m/s”. This statement, which is not further elaborated in Wieringa and Rijkoort (1983), has been used as the motivation and justification

for the use of the neutral stability assumption when dealing with wind measurements in the Netherlands.

As already discussed in Verkaik (2001, Section 5.5), if non-neutral conditions occur, but the stability and the planetary boundary layer height over the whole area would be the same, the WRTL model would still do very well. When the measuring height is 10 m, the effect of stability in the upwards transformation of the wind would to a large extent be cancelled by the downward transformation. However, if the atmosphere is stable (warm air over cold surface) at one location and unstable (cold air over warm surface) at another, the near-surface winds will be reduced at the former location and enhanced at the latter. Thus, if above water the situation would generally be instable and above land stable, then wind speeds above water would generally be higher than those above land. On the other hand, if above water the situation would generally be stable and above land instable, then the data would show the curvature problem,

Bottema and Van Vledder (2009) analysed seven years worth of wind data near and over Lake IJssel. They found that air-water temperature differences, an indicator of stability effects over open-water, had strong effects on spatial wind ratios, especially for weak winds, but to some extent even for gale-force winds. For the latter case they found that the curvature problem (and the model overprediction when extrapolating strong winds over land to open-water) becomes significantly stronger when stable conditions over open-water occur.

In this section we look for indications in the data whether stability does play a role at wind speeds above 6 m/s. And, if so, how does it influence the data. Before investigating the effects on the raw wind data (next sections), it was verified that stability effects did not affect the ECF estimates of Wever and Groen (2009). Within 2%, these effects could indeed be neglected (results not shown). Next, in Section 3.7.2 we look at the influence of stability on the ratios between coastal and inland wind speeds. In Section 3.7.3, case of the 25 of January 1990 storm (cf. Figure 12) is investigated in order to demonstrate that stability effects over open-water not only have significant effects for gale-force winds over lakes (as in Bottema and Van Vledder, 2009), but also during 10 Beaufort winds over sea.

3.7.2 Ratios between coastal and inland wind speeds

In order to check whether the gradient between the offshore and inland wind depends on stability, for a number of stations the ratio between the hourly averaged potential wind speed at a coastal station and at an inland station was computed and its dependence on the hour of the day plotted.

Figure 13 shows the ratio between the IJmuiden (coast) and Schiphol (land) wind speeds (see Figure 1 for their locations). The top panel shows the ratio of the measured wind speed and the bottom panel the ratio of the potential wind speed. To complement the information in Figure 13 and considering only winds coming from the coast:

- Figure 14 shows for each station, for wind speeds above 9 m/s, the wind speed variation with the time of the day.
- Figure 15 the wind speed ratios as function of the hour of the day and the season.
- Figure 16 the wind speed ratios as function of the hour of the day and a threshold applied to the data from the land station.

Figure 17 shows the same information as Figure 13 but for the Hoek van Holland (coast) and Soesterberg (land) stations. The equivalents of figures 14-16 for Hoek van Holland and Soesterberg (not shown), show similar features to those in figures 14-16.

In general it can be seen that the wind speed ratios have a minimum during the day, which is also slightly visible in wind speed at the coastal station (cf. figures 14 and 15). That in the land stations the variations of the mean wind speed along the day do not seem to be relevant (cf. figure 14). Furthermore, that for the highest potential wind speeds the ratios are lower than 1.1 (cf. figures 13 and 17).

As noted already by Bottema and Van Vledder (2009, p. 707) and Taminiau (2004) at some instants the ratio between the coast and the land wind speed is lower than one. Also, the

majority of the values below one seem to occur between 8 a.m. and 7 p.m., especially in the summer periods, although the same tendency is also present in the winter periods.

The ratio between the measured (raw) wind in Hoek van Holland and Soesterberg should, assuming the validity of the WRTL model, vary between 1.5 and 1.7 (Figure 9) and that is not the case for strong winds as shown in the top panel of Figure 17. The ratios of potential wind between coastal and land wind should, according to the neutral assumption, vary between 1.25 and 1.1 for high winds (between 20 and 27 m/s). That is also definitely not the case in the examples shown here. Note that as argued in Section 3.5 a part of the discrepancies found between the WRTL model ratios and those in the data can be attributed to the water roughness dependence on the wind speed. However, it does not provide the full explanation and what we argue here is that, since the ratios depend on the time of the day, differences in stability above water and inland also contribute to these discrepancies.

The temperature differences between the air mass and the sea water are not readily available for the coastal stations of Hoek van Holland and IJmuiden. Initial investigations with non quality controlled data from old stations (not shown) indicate that, as suggested by the time of the day plots, on average the land-sea wind speed ratio increases with increasing temperature difference between the air mass and the sea water. For a given water temperature, wind speeds over sea decrease with increasing air temperature because thermal stability increases, preventing exchange of momentum from higher levels. This is in line with the findings of Bottema (2007, figures 4.8 and 4.11) and Bottema and Van Vledder (2009, Figure 3).

3.7.3 Meteorological description of the January 1990 storm

From common synoptical and climatological knowledge one would expect maximum winds during storm events at coastal stations and not inland as one would expect wind to decrease with increasing roughness. The storm at January 25th 1990 shows the opposite. We have therefore analysed this storm in more detail.

During the storm the maximum potential wind speed was at Schiphol, reaching 27.0 m/s at 18 UTC. In fact, the open-water exposed station IJmuiden had a maximum potential wind speed of 25.6 m/s at 18 UTC, being smaller than at the nearby inland station Schiphol.

In a synoptical sense the wind field is part of a rapidly developing storm. With southwesterly winds mild air was advected in the warm sector around 12 GMT, air temperature about 12 °C, which was very mild for the end of January, see Figure 18. Even the colder air, coming to the Netherlands in the evening, is very mild and cools only to about 10 °C.

The water temperatures are remarkably colder. According to the 1990-1999 January average the water temperature is of about 5-6 °C in the Dutch North Sea coastal waters and of about 4 °C over the Lake IJssel region.

The contrast between air temperature and water temperature will lead to a stable air mass in a warm sector and just behind a cold front, in between 10 and 20 UTC. In stable conditions vertical exchange of momentum was reduced, resulting, especially during that time, to lower wind speeds over water and increased wind shear in the lower layers (lowest 1 km). Over warmer land areas vertical exchange of momentum will remain, leading to a relatively higher wind speed and less wind shear in the vertical wind profile.

The upper air measurements of temperature, pressure, humidity, wind speed and direction (not shown) were investigated and showed neutral conditions in vertical profiles over land. On the other hand, the colder sea water creates stable conditions in vertical profiles above the sea, the near-surface inversion (difference of temperature between the air mass and the sea surface) over water during the period of maximum wind speed (afternoon/evening) was in the order of 6 °C.

Trying to estimate the effect of stability on potential wind speed at 10 meter the wind-information from the soundings from De Bilt on the lowest standard level of 850 hPa was used, due to low surface pressure at a relative low altitude, approx. 1250 meters (at the

macro level). The objective is to look at relative differences; inferring the air/surface difference from the differences at 850 hPa. The ratio of this wind speed to wind at 10 meters in IJmuiden and Schiphol is calculated. In Figure 19 the difference between these ratios is shown in blue. The difference between the temperature at 850 hPa and at a height of 1.5 meters are shown for Schiphol in purple and for IJmuiden in yellow.

During the day (and thus in different stability situations) an increase in the difference of the ratios is established at 18 UTC, the time that the mild air is still present at both stations (just behind the coldfront). Note that the upper air measurements are executed every 6 hours, and a subjective interpolation of the wind and temperature graphs is therefore necessary. Maximum vertical temperature difference at IJmuiden is estimated 6 to 7 °C from 12 to 18 UTC.

In conclusion, the following can be said about the effect of the stability due advection of warm air over cold water on potential wind. In specific storm events like January 25th 1990 with advection of warm air over cold water, potential wind speeds at sea and coast might be reduced in the order of 2 to 3 % per degree temperature inversion.

The estimate of the influence of the wind speed reduction in atmospheric stable conditions (warm air over cold water) with potential wind speeds of 25 m/s is in agreement with Figure 4.11 of Bottema (2007), who estimated a reduction in wind speed due to stability from the wind ratio IJsselmeer/Schiphol of about 7%, 5% and 3% per (positive) degree T_{air}-T_{water} for wind speeds of reps. 8 m/s, 12 and 16 m/s. Furthermore, preliminary results for the North Sea (as discussed in Section 3.7.2) do not contradict Bottema (2007) findings.

3.7.4 Summary

To recap, the analyses presented in this section indicate that:

- For high wind speeds the ratio between coastal and land potential wind is about 20% lower than the estimates from the WRTL model. The lower ratios seem to be a consequence of differences in the stability at the coast and above land.
- In typical southwesterly storms with a significant warm sector, like the January 1990 storm, during the period of the storm maxima stability in the warm sector, temporal changes due to warmer air mass over colder sea water cause thermal stability and a decrease of wind speed over sea/coast, estimated at about 2 to 3 % per degree of temperature difference at wind speeds above 15 m/s to 5-7% for wind speeds around 10 m/s.

4. Conclusions and recommendations

This paper defines the so-called curvature problem as the discrepancy between the modelled and measured strong wind speed ratios of open-water locations and KNMI land-based reference stations, respectively. We used the Wieringa and Rijkoort (1983; also Wieringa 1986) Two-Layer (WRTL) model, which reduces to the theoretical framework of logarithmic wind profile and resistance law if the terrain around each of the locations is sufficiently uniform. In this study we have identified the effects of the assumptions made in

a) the standardization of the measured wind speeds into (so-called potential) wind speeds corrected for local exposure effects and in
b) the translation of these to 10 m wind speeds to other, especially open-water, locations.

We here summarize our conclusions using a separation into two classes. The first class considers the conclusions with respect to some of the assumptions in the wind modelling concept, the second concerns the potential wind speed data.

For each source we give an estimate of how it may affect the ratio of the sea-land wind speed at the high wind speed considered in the respective analysis (around 25 m/s). Given that at low wind speeds the observed sea-land wind speed ratios seem to be on average close to those according to the WRTL model and at high wind speeds lower, the effect of the considered source at high wind speeds gives an idea of the effect in the curvature problem (a deviation from a (approximately) constant ratio for all return values). The values provided can, therefore, be used to approximately rank the importance of each possible source.

With respect to some aspects in the wind modelling concept the following conclusions can be drawn:

- *Wind speed dependent water roughness*
  The fact that the water surface roughness is not constant but depends on (a.o.) the wind speed provides a significant but no dominant part of the explanation for the above-described curvature problem. It should be taken into account in the interpretation of measurement data, but it also complicates the interpretation and use of the concept of potential wind.
  Furthermore, in the homogenisation of the series of measurement data, a wind speed independent exposure correction factor is applied. The actual water roughness, which the factor is supposed to correct for, does depend on the wind speed. Neglecting the wind speed dependence in water roughness and in the determination of the potential wind series, both enhance the difference in curvature. The effect on the sea-land wind speed at high wind speeds is systematic and up to about 30%.
- *Non-neutral atmospheric stability*
  The assumption of a neutral atmospheric stability for all conditions in which the wind speed exceeds 6 m/s appears to be invalid with advection over sea of warm air over cold water, even for the highest observed wind speeds This implies that the (shape of the) wind speed profile is not guaranteed "logarithmic and governed by surface roughness only". The inclusion of coastal stations in the analysis and the spatial translation from land stations to water locations without modelling atmospheric (thermal) stability complicates the use and interpretation of the concept of 'potential wind'. Thermal stability effects above water can affect the sea-land wind speed ratio at high wind speeds by a much as 20%, but it is not yet known how systematic it is.
- *Storm dynamics*
  An analysis of the simultaneous occurrence of the highest extremes at the considered stations, has shown that especially extreme storms can be rather localized and the stations affected by a certain storm can vary substantially from storm to storm. This indicates that spatial variations of the geostrophic wind and temporal variations of the pressure fields (causing isallobaric winds) are not uncommon in extreme storms. The model assumption of a constant geostrophic wind between two stations at a certain distance (not quantified yet) does not properly describe such storms. The effect of storm dynamics on the sea-land wind speed at high wind speeds is not systematic, but for certain storms can be as much as about 20%.

Uncertainties have been identified in the data, which influence the quality of the data:

- *Inhomogeneities*
  The potential wind time series sometimes contain some inhomogeneities: jumps and trends. Furthermore, a relationship was found between trends in potential wind and trends in exposure correction factors. If this indicates changes in meso-scale roughness, this can have a strong impact in the way potential wind is used in extreme wind statistics. Our estimate is that inhomogeneities do not systematically affect the sea-land wind speed. Nevertheless, in certain circumstances, they may affect it by as much as 5%.
- *Non-stationary anemometer height*
  Certain coastal stations, e.g. at Hoek van Holland and IJmuiden, are exposed to the sea in a sea-to-land flow. It is expected that when high surges accompany extreme sea wind, which is a common situation, that the considered height of anemometer relatively to the mean sea level is an overestimation of the effective measuring height and the computed potential wind an underestimation. According to our computations, the effect on the sea-land wind speed at high wind speeds is systematic and at most 5%, provided that the atmosphere is neutral. However, in non-neutral (especially stable) atmospheres the effects of anemometer heights deviating from the regular 10 m, whether due to

measuring site characteristics or surge- and tide-related water level variations, can be considerably larger (Verkaik, 2000, Fig.12).

From the analyses in this study and the conclusions drawn from them, it can be concluded that valuable insight is obtained in the (likely) sources of the curvature problem, i.e. the disagreement between the data and the wind modelling concept. In fact, the curvature problem appears to have a *combination* of causes instead of just a single cause. The identified causes seem to be located in fairly fundamental aspects of both the available data and the present wind modelling concept.

Our main conclusion is thus that the curvature problem is a real phenomenon which is, to a large extent, related to fundamental aspects of both the available data and the present wind modelling.

Acknowledgments

The presented work is part of the SBW (Strength and Loads on Water Defenses) project commissioned by Rijkswaterstaat Centre for Water Management in the Netherlands. The authors would also like to thank Arnout Feijt and Albert Klein Tank for their helpful comments on this work.

References

Beljaars, A. C. M., 1988: *The measurement of gustiness at routine wind stations - a review*. WMO-TECO-1988. Leipzig. pp. 311–316. WMO/TD-No. 222, also Royal Netherlands Meteorological Institute, Sc. Rep., WR 87-11.

Bottema, M., 2007: *Measured wind-wave climatology Lake IJssel (NL). Main results for the period 1997-2006*. Report RWS RIZA 2007.020, July 2007 (http://english.verkeerenwaterstaat.nl/kennisplein/3/5/359788/Measured_wind-wave_climatology_lake_IJssel_(NL)-main_results_for_the_period1.pdf).

Bottema, M., W. Klaassen and W.P. Hopwood, 1998: Landscape roughness parameters for Sherwood Forest. *Boundary-Layer Meteorol.*, 89, pp. 285–316.

Bottema, M. and G. Ph. van Vledder, 2009: A ten-year data set for fetch- and depth-limited wave growth. *Coastal Engineering*, 56 (7), pp. 703-725.

Businger, J. A., J. C. Wyngaard, Y. Izumi and E. F. Bradley, 1971: Flux-Profile Relationships in the Atmospheric Surface Layer. *J. Atmos. Sci*., 28, pp. 181–189.

Caires, S., 2009: *Extreme wind statistics for the Hydraulic Boundary Conditions for the Dutch primary water defences*. SBW-Belastingen: Phase 2 of subproject 'Wind modelling'. Deltares Report 1200264-005.

De Haij, M., 2009: *Automatische validatie van druk- en windwaarnemingen op het KNMI - een verkenning* (In Dutch). KNMI Intern report 2009-3 (http://www.knmi.nl/bibliotheek/knmipubIR/IR2009-03.pdf).

De Waal, J.P., 2003: *Windmodellering voor bepaling waterstanden en golven. Een analyse van de bouwstenen* (In Dutch). RIZA werkdocument 2003.118x, 60 p., RWS RIZA (http://english.verkeerenwaterstaat.nl/kennisplein/1/7/178030/2003.118X.pdf).

Dillingh, D., L. de Haan, R. Helmers, G.P. Können and J. van Malde, 1993: *De basispeilen langs de Nederlandse kust; statistisch onderzoek* (In Dutch). Rijkswaterstaat, Dienst Getijdenwateren /RIKZ, Report DGW-93.023 (http://english.verkeerenwaterstaat.nl/kennisplein/2/1/215184/DGW%2093023A.pdf).

Frenzen, P. and Vogel, C. A., 1995: On the magnitude and apparent range of variation of the von Karman constant in the atmospheric surface layer. *Bound.-Layer Meteor*., 72, pp. 371–392.

Foken, T.,2006: 50 Years of Monin-Obukhov similarity theory. *Boundary-Layer Meteorology*, 119, pp. 431-447.

Garrat, J. R., 1992: *The Atmospheric Boundary Layer*. Cambridge Univ. Press.

Komen, G. J., L. Cavaleri, M. Donelan, K. Hasselmann, S. Hasselmann and P. A. E. M. Janssen, 1994: *Dynamics and Modelling of Ocean Waves.* Cambridge Univ. Press.

Rijkoort, P. J., 1983: *A compound Weibull model for the description of surface wind velocity distributions*. Scientific Report, WR 83-13, Royal Netherlands Meteorological Institute (KNMI).

Smits, A., A. M. G. Klein Tank and G. P. Können, 2005: Trends in storminess over the Netherlands, 1962-2002. *Int. Journal of Climatology*, 25 (10), pp. 1331-1344.

Taminiau, C., 2004: *Wind (extremen) in het IJsselmeergebied* (In Dutch). RIZA werkdocument 2004.138x, 60 p., RWS RIZA.

Tennekes, H., 1973: The logarithmic wind profile, *J. Atm. Sci*., 30, pp. 234-238.

Tieleman, H. W., 2008: Strong wind observations in the atmospheric surface layer. *J. Wind Eng. Ind. Aerodyn.*, 96, pp. 41–77.

Troen, I. and E.L. Petersen, 1989: *European Wind Atlas*. Risø National Laboratory, Roskilde. 656 pp.

Vautard, R., J. Cattiaux, P. Yiou, J.-N. Thépaut and P. Ciais, 2010: Northern Hemisphere atmospheric stilling partly attributed to an increase in surface roughness, *Nature Geosci*., 3, pp. 756–761, doi:10.1038/ngeo979

Verkaik, J.W., 2000: Evaluation of Two Gustiness Models for Exposure Correction Calculations. *J. of Appl. Meteor*., 39 (9), pp. 1613–1626.

Verkaik, J.W., 2001: *A method for the geographical interpolation of wind speed over heterogeneous terrain*. KNMI (http://www.knmi.nl/samenw/hydra/documents/geograph/index.html).

Verkaik, J.W., 2006. *On Wind and Roughness over Land*. Ph. D. Thesis, Wageningen University, The Netherlands, 123p. (http://edepot.wur.nl/121786)

Verkaik, J. W., A. Smits and J. Ettema, 2003a: *Wind climate assessment of the Netherlands 2003: Extreme value analysis and spatial interpolation methods for the determination of extreme return levels of wind speed*. KNMI-HYDRA project Phase report 9. KNMI (http://www.knmi.nl/samenw/hydra/documents/phasereports/ph09.pdf).

Verkaik, J. W., A. Smits and J. Ettema, 2003b: *Naar een nieuwe extreme waardenstatistiek van de wind in Nederland* (In Dutch). KNMI-HYDRA project Phase report 16. KNMI (http://www.knmi.nl/samenw/hydra/documents/phasereports/ph16.pdf).

Wever, N and G. Groen, 2009: *Improving potential wind for extreme wind statistics*. KNMI Scientific Report WR2009-02, March 2009 (http://www.knmi.nl/bibliotheek/knmipubWR/WR2009-02.pdf).

Wieringa, J., 1986: Roughness-dependent geographical interpolation of surface wind speed averages. *Quart. J. Royal Meteor. Soc.*, 112, pp. 867-889.

Wieringa, J., 1992: Updating the Davenport roughness classification. *J. Wind Eng. Ind. Aerodyn.*, 41-44 , pp. 357-368.

Wieringa, J., 1993: Representative roughness parameters for homogeneous terrain. *Boundary-Layer Meteorol.*, 63, pp. 323–363.

Wieringa, J., 1996: Does representative wind information exist? *J. Wind Eng. Ind. Aerodyn.*, 65, pp. 1-12.

Wieringa, J. and P. J. Rijkoort, 1983: *Windklimaat van Nederland* (In Dutch). Staatsdrukkerij, 's Gravenhage (NL).

Table(s)

Station name	Anemometer height (m)	Period of available data	Trends in the U_m annual mean (cm/s/yr)	Trends in the U_p annual mean (cm/s/yr)
IJmuiden	18.5	1952-2009	2.9	1.0
Texelhors	10.0	1969-2009	-1.9	-1.2
De Kooy	10.0	1972-2009	–	–
Schiphol	10.0	1950-2009	–	–
DeBilt	20.0	1961-2009	–	-2.7
Soesterberg	10.0	1958-2008	–	–
Leeuwarden	10.0	1961-2009	–	–
Deelen	10.0	1961-2009	-1.5	–
Lauwersoog	10.0	1968-2009	-1.0	–
Eelde	10.0	1961-2009	–	1.2
Twenthe	10.0	1970-2009	1.9	1.8
Cadzand	17.1	1972-2009	-1.9	-1.9
Vlissingen	27.0	1959-2009	1.6	–
L.E. Goeree	38.3	1951-2009	2.3	–
Hoek van Holland	15.0	1962-2009	2.2	–
Zestienhoven	10.0	1961-2009	–	0.6
Gilze-Rijen	10.0	1961-2009	-1.1	–
Herwijnen	10.0	1965-2009	–	–
Eindhoven	10.0	1960-2009	-1.1	–
Volkel	10.0	1971-2009	–	1.5
Beek	10.0	1961-2009	1.5	1.0

Table 1 Trends in cm/s/yr in the measured and potential wind annual mean of values above 5 m/s. Only the trends that were found significant at a 5% level are shown.

	U_m (m/s)	10	15	20	25	30
		ECF_{SWL}/ECF				
α=0.018	SWL=3 m	1.0212	1.0236	1.0256	1.0275	1.0293
	SWL=5 m	1.0395	1.0439	1.0478	1.0515	1.0550
α=0.032	SWL=3 m	1.0229	1.0256	1.0281	1.0305	1.0329
	SWL=5 m	1.0425	1.0478	1.0527	1.0574	1.0620

Table 2 Effect in the ECF of considering a SWL other than 0.

T year	$U_{pc,A}$ m/s	$U_{pc,B}$ m/s	remark
-	8.0	10.8	read from Fig. 2 (Dots)
-	9.0	12.1	
-	10.0	13.3	
-	11.0	14.4	
-	12.0	15.6	
-	13.0	16.6	
-	14.0	17.5	
-	15.0	18.2	
0.5	15.6	18.7	read from Fig. 2 (Lines) (also available as tabulated statistics)
1	17.0	19.8	
2	18.3	20.7	
5	19.9	21.8	
10	21.1	22.5	
20	22.2	23.2	
50	23.5	24.0	
100	24.5	24.5	
200	25.5	25.0	
500	26.7	25.7	
1000	27.5	26.1	
2000	28.4	26.5	
5000	29.5	27.0	
10000	30.3	27.3	

Table 3 Potential wind speeds U_{pc} at Soesterberg (A) and Hoek van Holland (B) at identical recurrence intervals (T).

Figure(s)

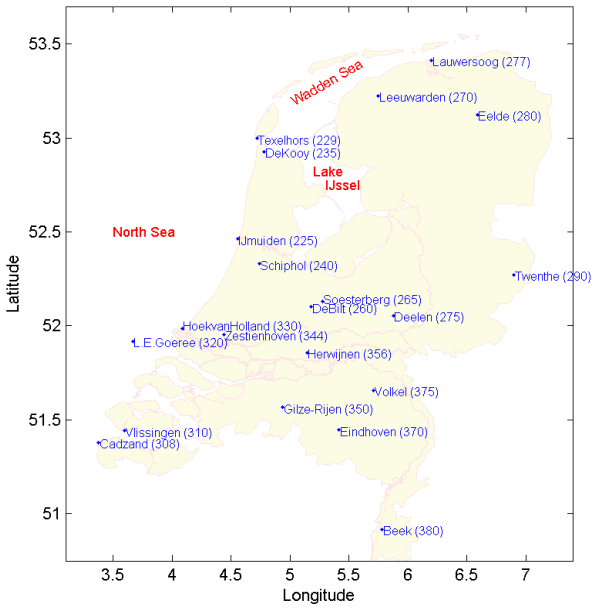

Figure 1 Location name and reference number of the KNMI wind stations in which long term measurements are available.

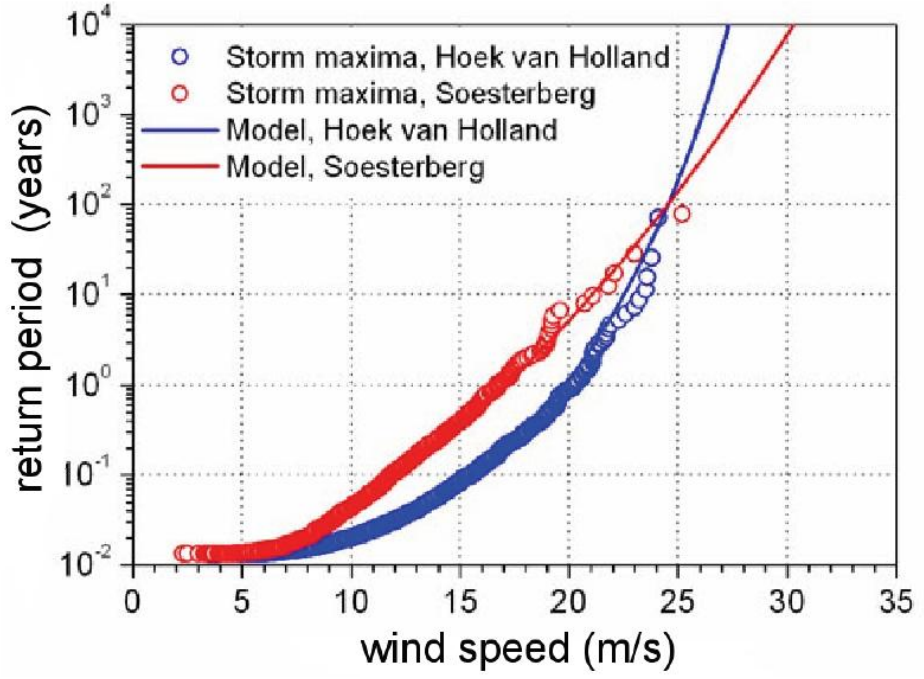

Figure 2 Potential wind speed maxima above 2 m/s distancing at least 48h from each other and the KNMI-Hydra project (Verkaik et al., 2003a) fits to the data extremes for stations Hoek van Holland (a coastal station) and station Soesterberg (a land station). The empirical return periods were computed using the Gringorten (1963) plotting positions. Figure taken from Verkaik et al. (2003b).

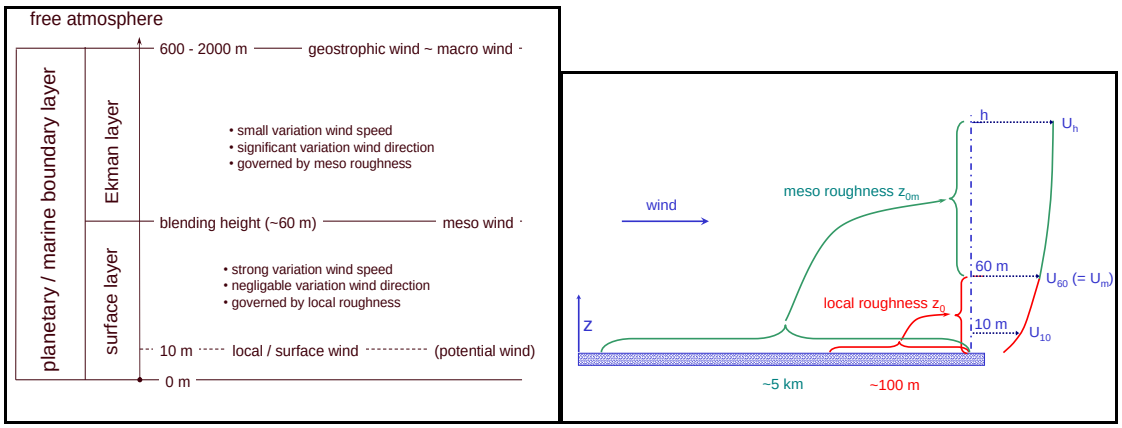

Figure 3 Left panel: Schematized properties of the wind in the two-layer model. Right panel: Relation between surface roughness and the wind speed profile, subdivided in two layers.

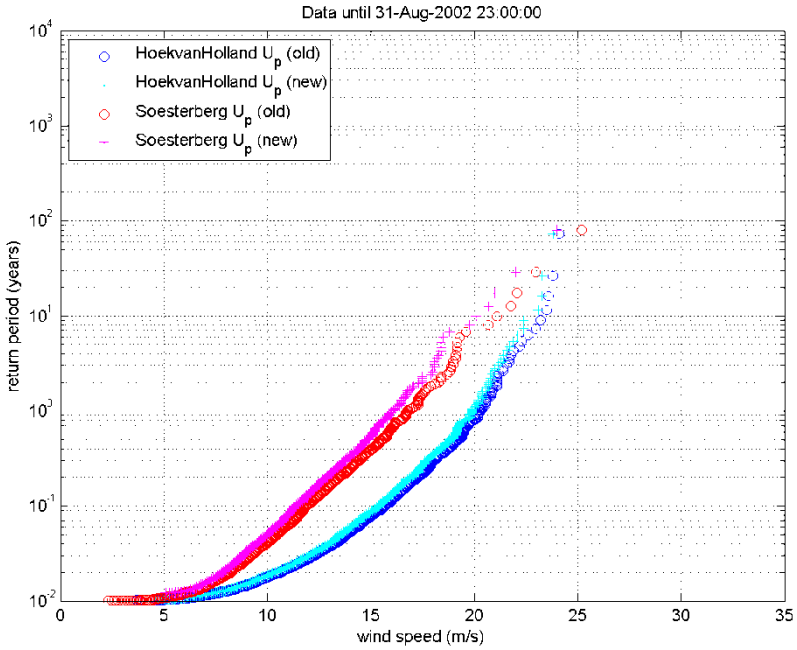

Figure 4 Reproduction of the KNMI-Hydra project figure (cf. Figure 2) using the old and new potential wind time series and no data fits. The empirical return periods were computed using the Gringorten (1963) plotting positions.

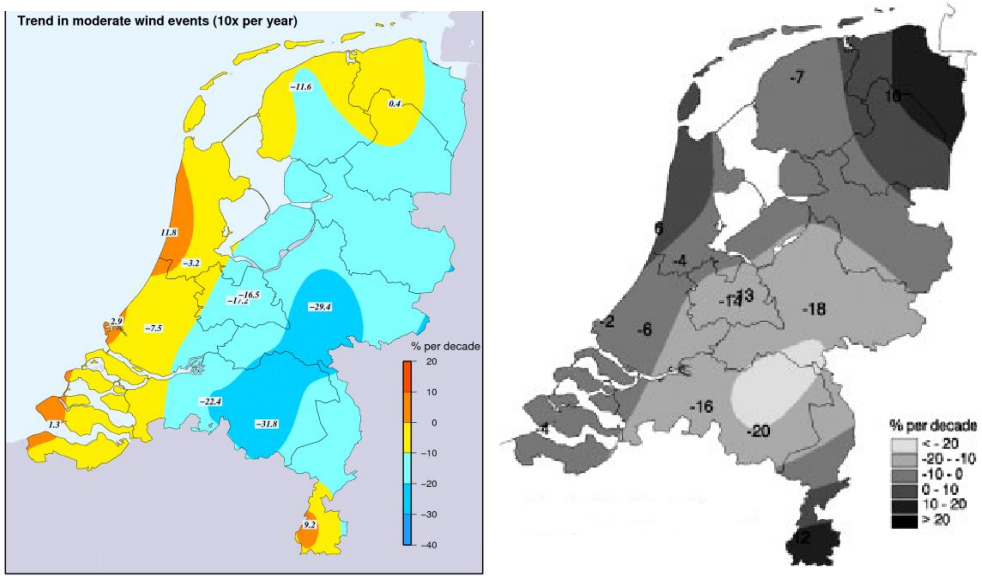

Figure 5 Trends in moderate wind events. Left panel: This study. Right panel: Figure taken from Smits et al. (2005).

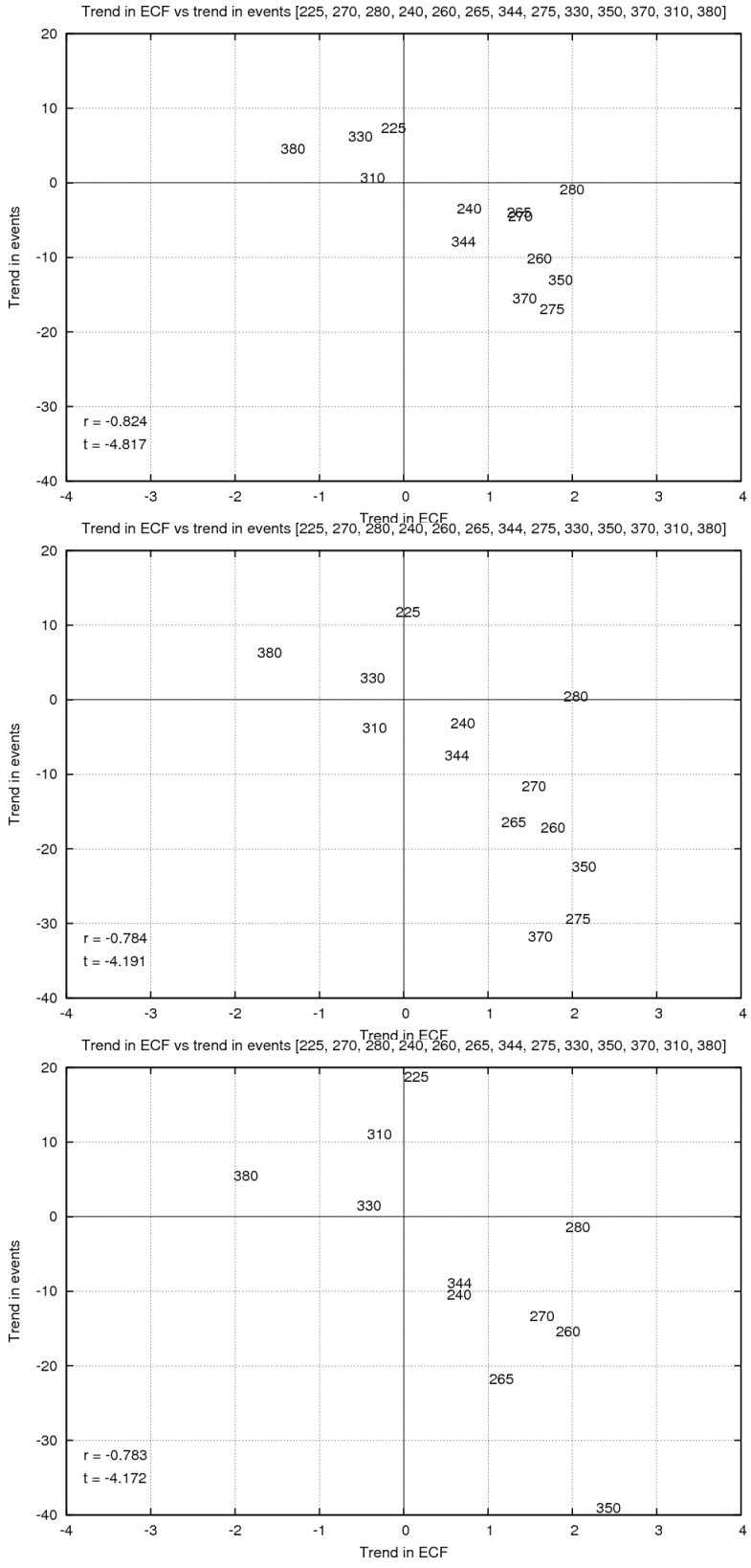

Figure 6 Trends in weak (top panel), moderate (middle panel) and strong (bottom panel) wind events versus the directional weighted trend in exposure correction factors. Trends are given as a percentage per decade. Numbers shown denote KNMI station numbers. Note that in the bottom panel two stations do not fit on the vertical scale and are not shown.

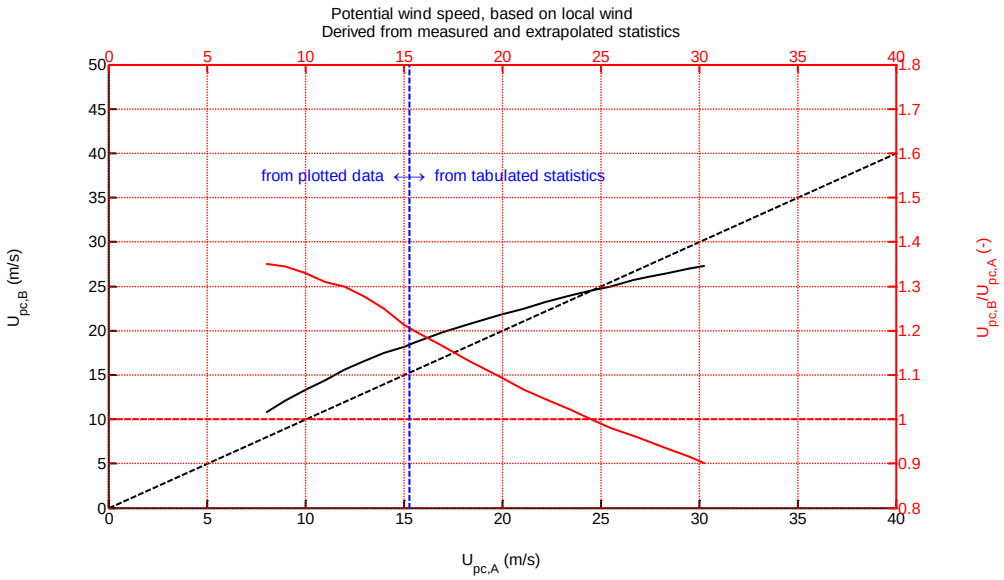

Figure 7 Relation between the potential wind speeds U_{pc} at Soesterberg (A) and Hoek van Holland (B) at identical recurrence intervals (T). (The colour of the lines refers to the color of the associated y-axis).

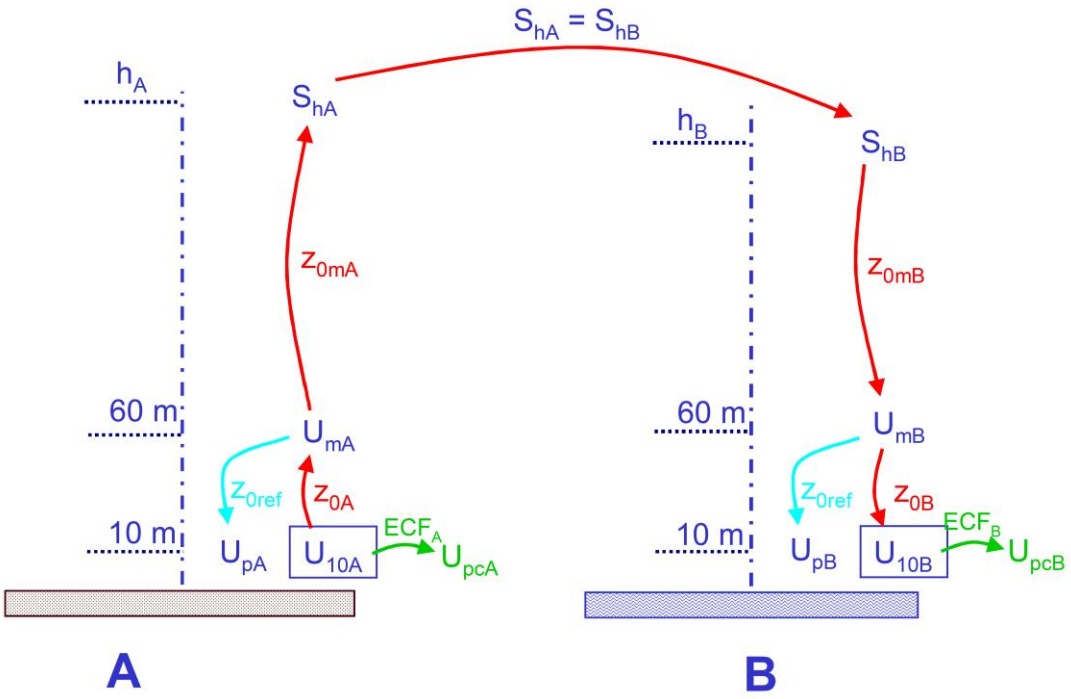

Figure 8 Schematic procedure to assess the relationship between the local wind speeds at location A and B (red arrows), between the potential wind speeds based on meso wind at location A and B (red and turquoise arrows) and between the potential wind speeds based on local wind at location A and B (red and green arrows), using the Wieringa-Rijkoort two-layer model.

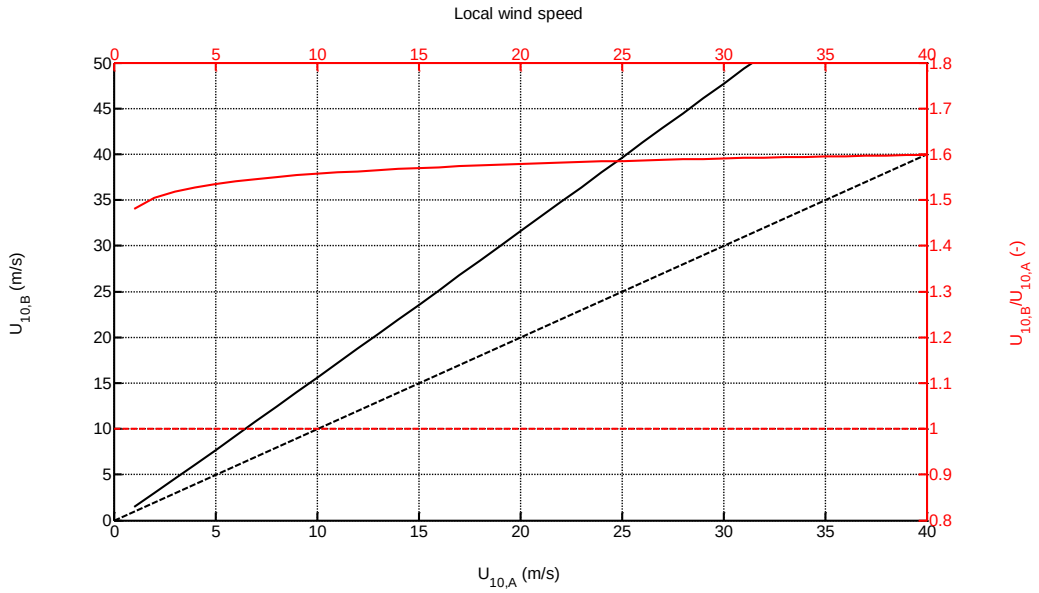

Figure 9 Reference computation: relationship between the local wind at locations A and B for a small but constant (wind speed independent) water roughness.

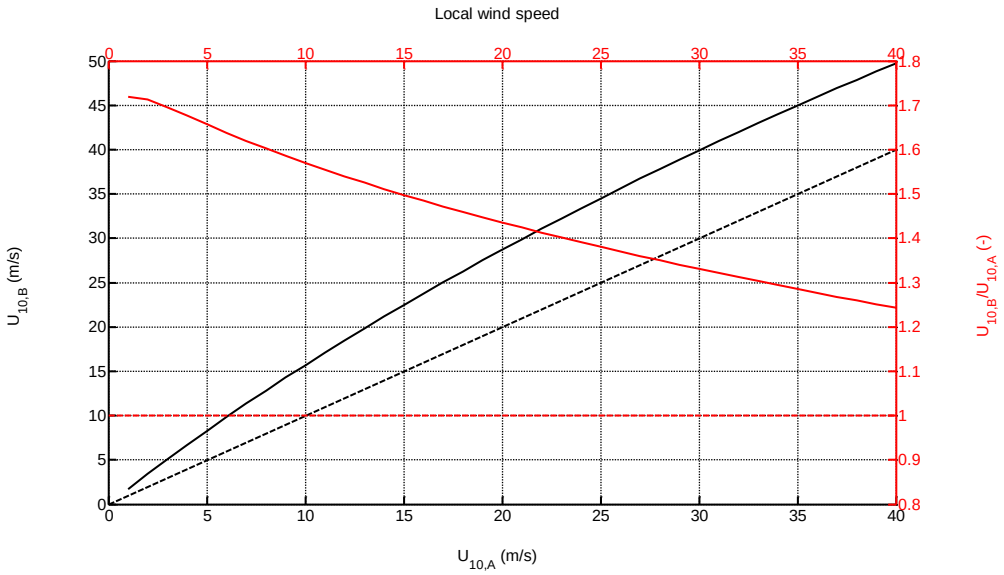

Figure 10 Computed relationship between the local wind at locations A and B for wind speed dependent water roughness (for α=0.032).

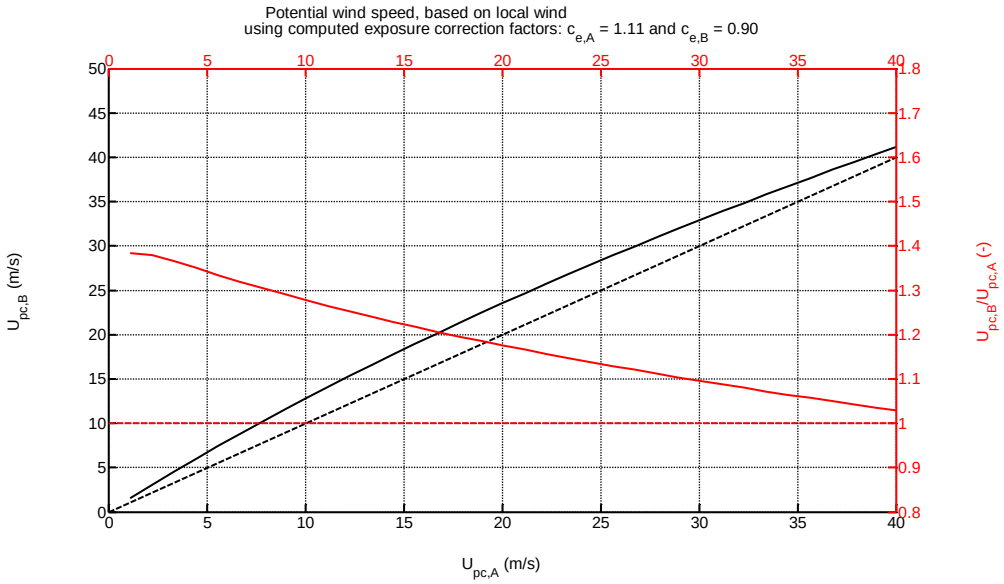

Figure 11 Computed relationship between the potential wind (based on local wind) at locations A and B.

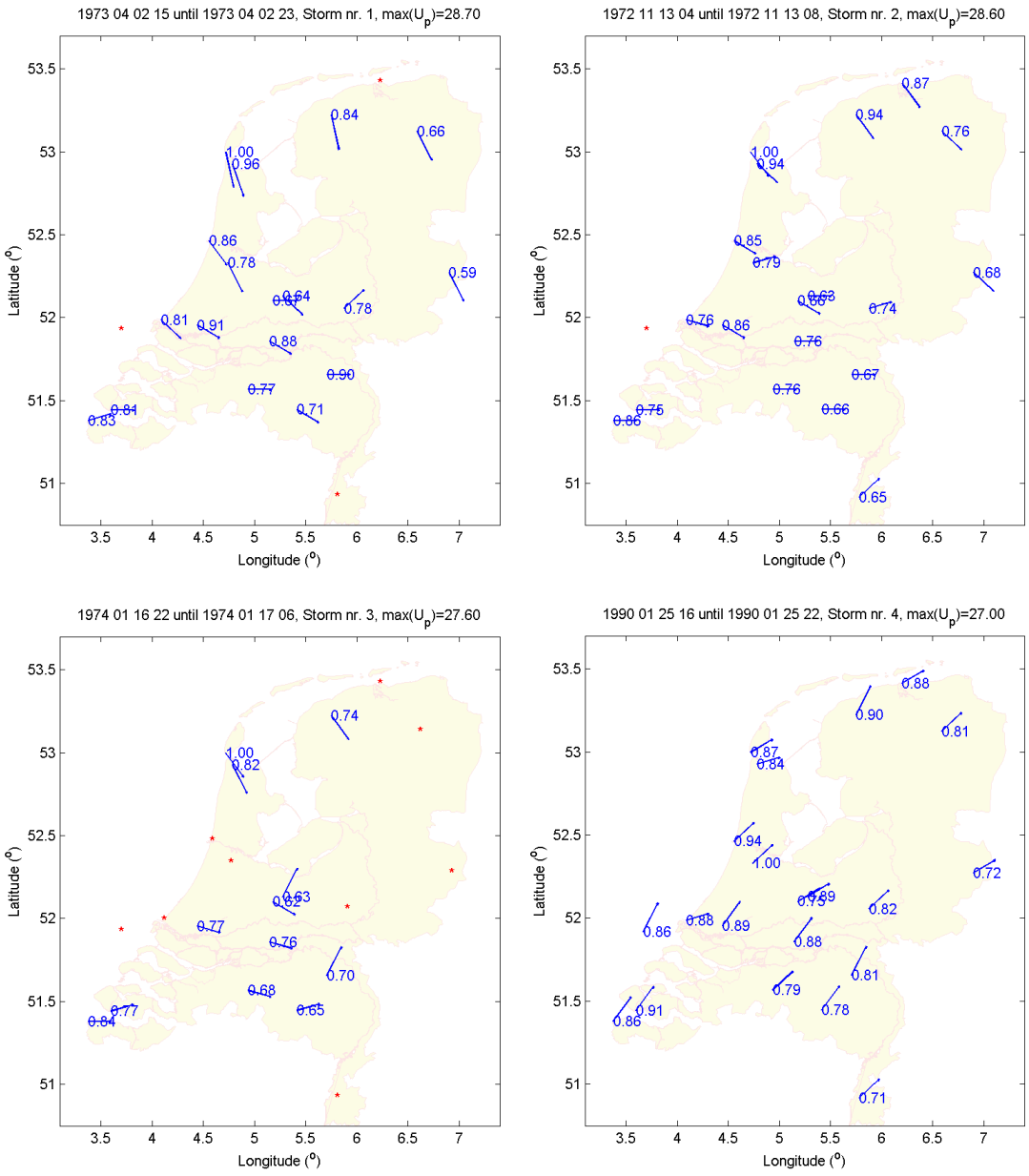

Figure 12 The highest four potential wind speed storms. The storms were ranked in terms of the maximal potential wind speed within the storm.

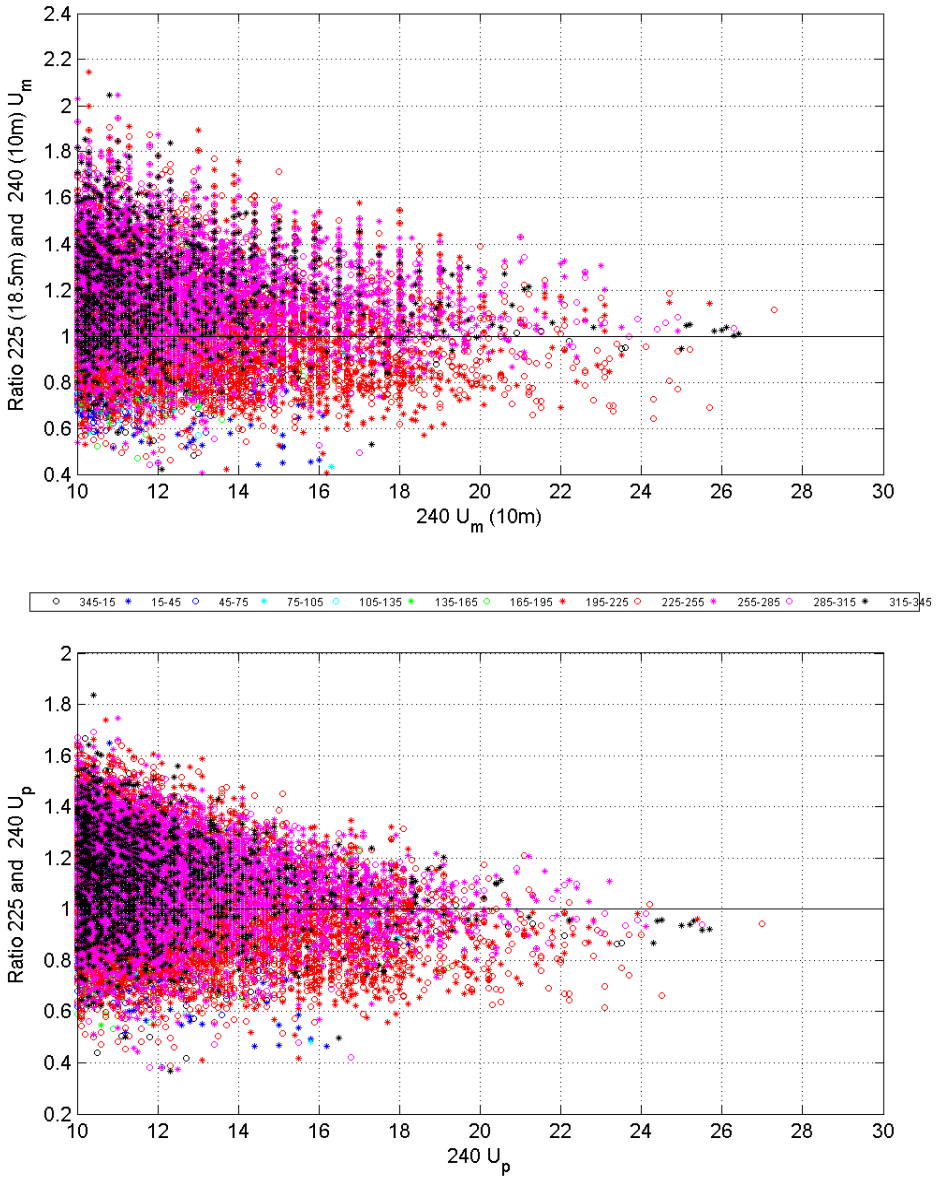

Figure 13 IJmuiden (225, 18.5 m) vs Schiphol (240, 10 m). Top panel: Ratio between the measured wind. Bottom Panel: Ration between the potential wind. Period: 1/4/1952 until 4/4/2009.

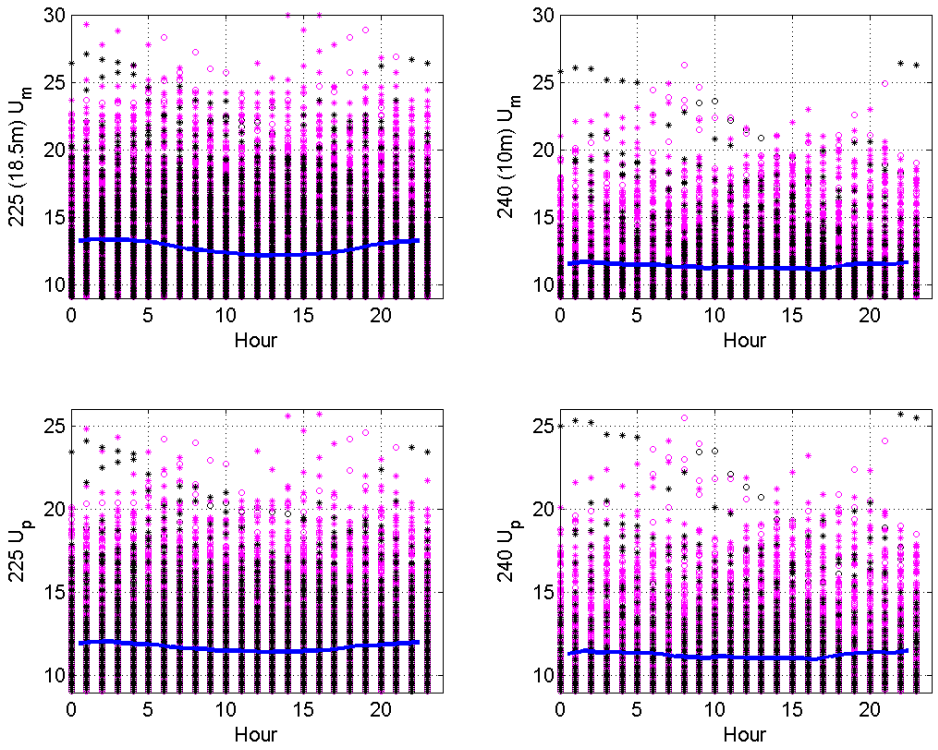

Figure 14 Variation with the time of the day of the IJmuiden (225, left panels) and Schiphol (240, right panels) measured (top panels) and potential (bottom panels) wind speed. Only for dates when the wind direction in IJmuiden (the coastal station) varies between 255ºN and 15ºN and using a threshold of 9 m/s per panel. Period: 1/4/1952 until 4/4/2009. The blue lines indicate the hourly means (above 9 m/s).

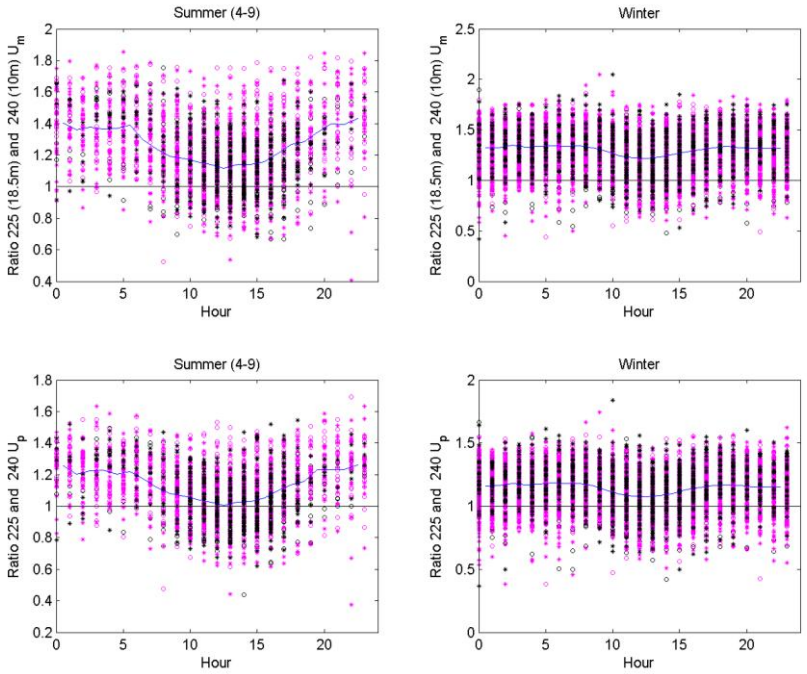

Figure 15 Variation with the time of the day of the ratio between the IJmuiden (225, 18.5 m) and the Schiphol (240, 10 m) measured (top panels) and potential (bottom panels) wind speed Summer (left panels) and Winter (right panels). Only for dates when the wind direction in IJmuiden (the coastal station) varies between 255ºN and 15ºN. Period: 1/4/1952 until 4/4/2009. The blue lines indicate the hourly means.

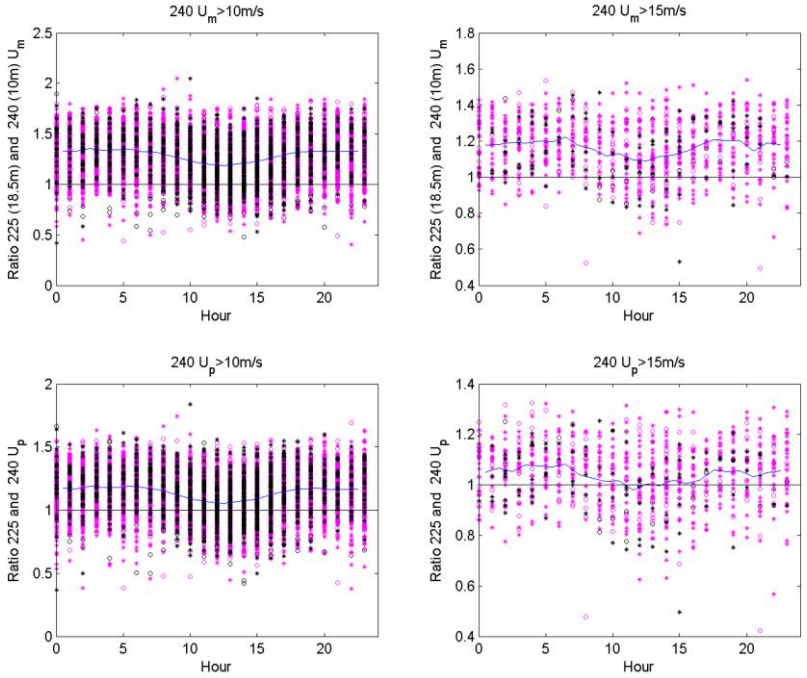

Figure 16 Variation with the time of the day of the ratio between the IJmuiden (225, 18.5 m) and the Schiphol (240, 10 m) measured (top panels) and potential (bottom panels) wind speed applying a 10 m/s (left panels) and 15m/s (right panels) threshold to the data from the Schiphol (land) station. Only for dates when the wind direction in IJmuiden (the coastal station) varies between 255ºN and 15ºN. Period: 1/4/1952 until 4/4/2009. The blue lines indicate the hourly means.

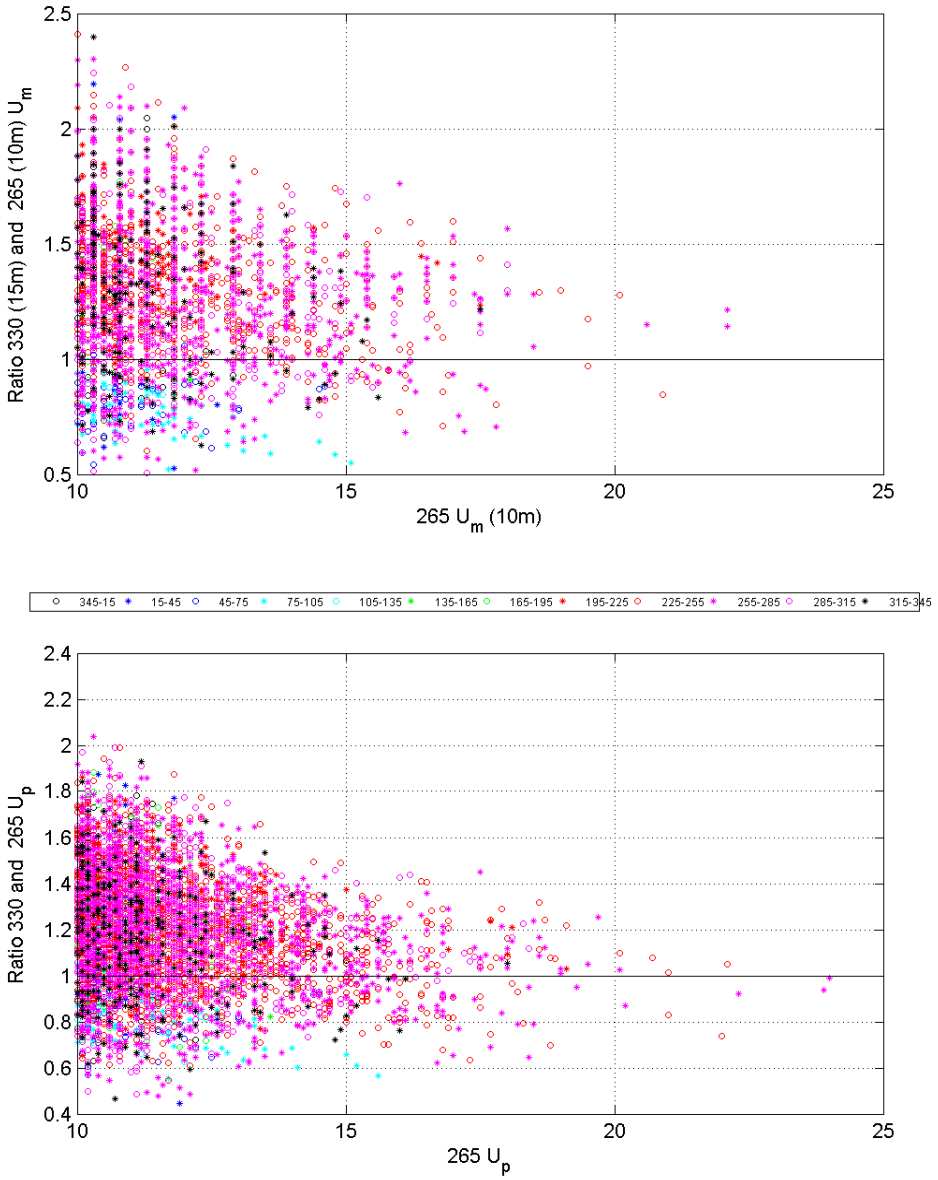

Figure 17 Hoek van Holland (330) vs Soesterberg (265). Top panel: Ratio between the measured wind. Bottom Panel: Ration between the potential wind. Period: 1/1/1962 until 16/11/2008.

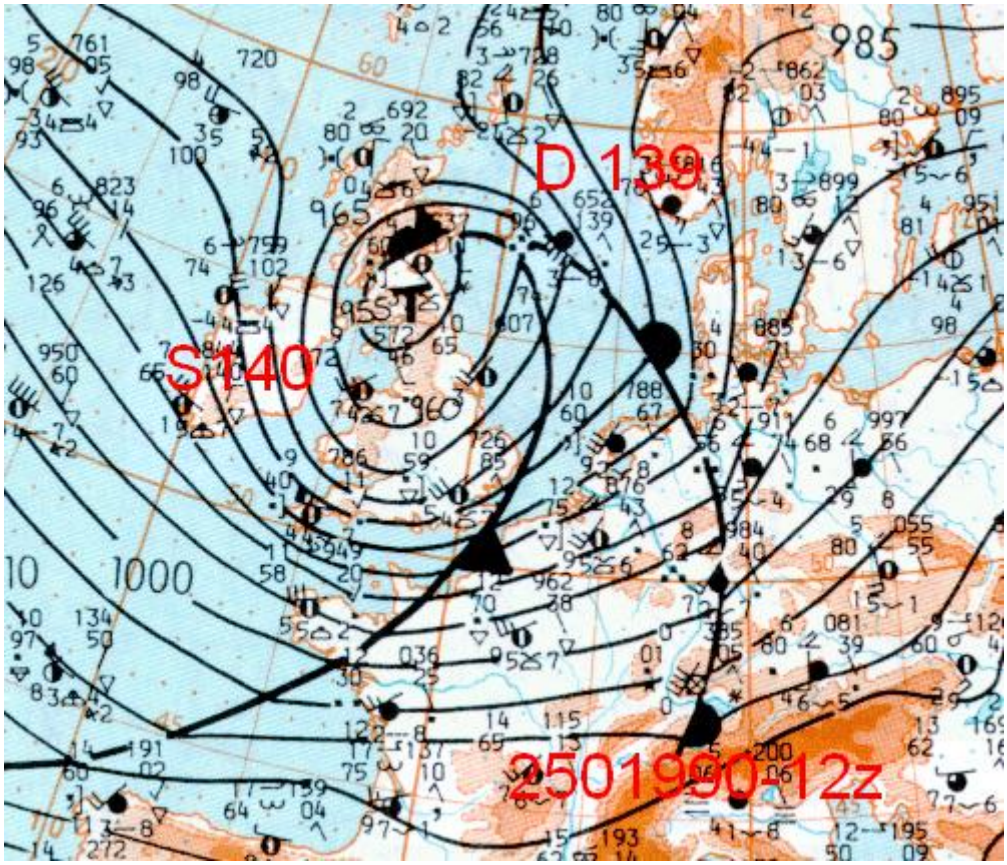

Figure 18 Synoptic weather chart of 25 January 1990, 12 UTC. Low pressure centre 953 hPa over Scotland, warm sector over central North Sea and Netherlands to the south. Strong southwesterly winds advect mild air over cold seawater to the Dutch coast.

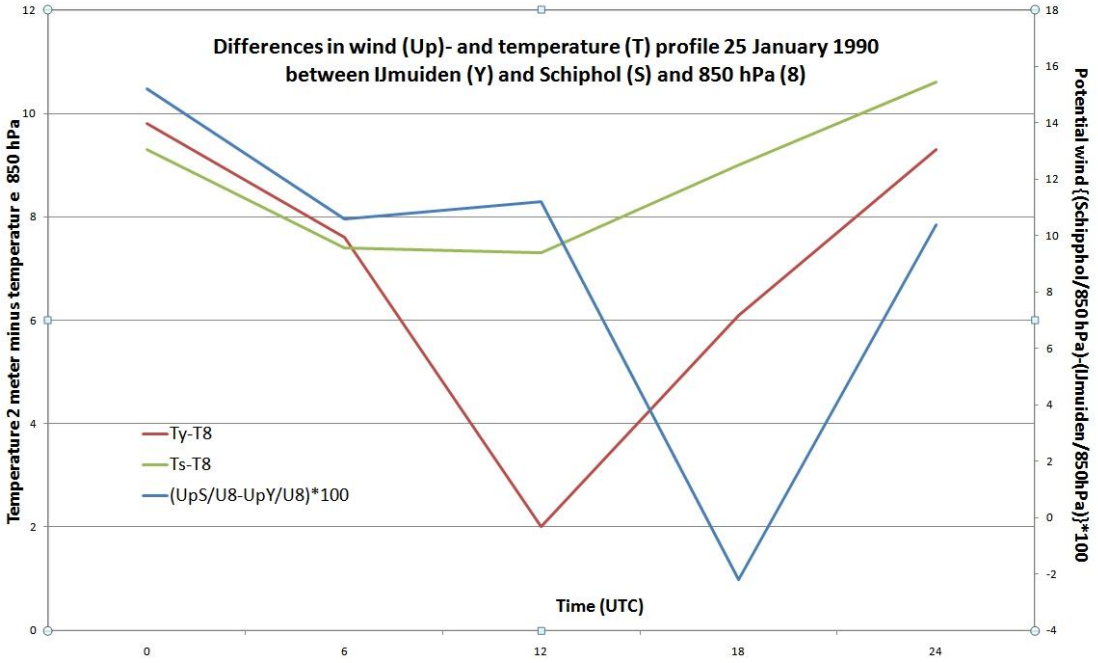

Figure 19 Difference in ratios wind 10 meters and 850 hPa (1250 meters) at IJmuiden and Schiphol (blue), temperature differences 850 hPa and 1.5 meters at Schiphol (green) and IJmuiden (red).